Chapter 5

Propagation Characteristics of Surface Discharge under Impulse Application Voltage

5.1 Introduction

Flashover on insulator surface in air at atmospheric pressure occurs as a sequence of several processes that leads to the formation of a plasma channel which bridges the electrode gap. The main stages of the flashover are the occurrence of initial seeding electrons, the development of electron avalanches, the inception and the propagation of streamers, the streamer-to-leader transition, the propagation of leader, and the formation of a breakdown[1, 2]. The streamer-to-leader transition is a very critical stage of such a breakdown since the leader can propagate a long distance with a low increment of application voltage. The streamer-to-leader transition and the propagation process of a leader are still the object of intensive experimental and theoretical studies [3, 4, 5, 6].

In this chapter, the propagation characteristics of surface discharge including propagation speed, length, and the residual charge distribution are investigated under the application of impulse voltage with the 2-layer structure pipe, where the surface discharge propagates on the pipe without any accumulated charge.

5.2 Propagation Length of Surface Discharge

The propagation length of impulse surface discharge on the 2-layer structure pipe is measured with changing the applied voltage. The distance between electrodes, *d*, is set to 100 mm, and 300 mm, and the experiments under each impulse voltage are repeated four times.

Figures 5.1 and 5.2 show the relationships between the propagation length, which are measured from the photographs, and the peak values of the application voltage for d = 100 mm and 300 mm, respectively. The experimental conditions are shown respectively in Table 5.1 and 5.2.

For the positive discharge when d = 100 mm, the discharge distance can be fitted by

the following equation:

$$L_P = 0.00010\, V_P^{4.8} \tag{5.1}$$

For the negative discharge when d = 100 mm, the discharge distance can be fitted by the following equation:

$$L_N = 0.011\, V_P^{2.8} \tag{5.2}$$

For the positive discharge when d = 300 mm, the discharge distance can be fitted by the following equation:

$$L_P = 0.019\, V_P^{4.8} \tag{5.3}$$

For the negative discharge when d = 300 mm, the discharge distance can be fitted by the following equation:

$$L_N = 0.012\, V_P^{2.8} \tag{5.4}$$

Discharge length of surface discharge under impulse voltage application for electrodes distance d = 100 mm and d = 300 mm are put together for comparison to study the influence of electrodes distance on the discharge length of surface discharge, as shown in Fig. 5.3.

The electrodes distance has little influence to the discharge length for negative impulse discharge, while it has a big influence to the discharge length for positive impulse discharge.

Table 5.1 Experimental condition for Fig. 5.1

Insulator	Two-layer structure pipe
Back electrode	Grounded
Distance between ring electrodes	d = 100mm
Application Voltage	Impulse

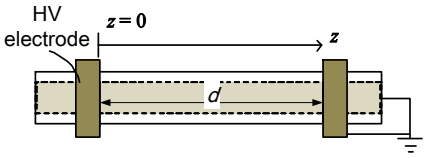

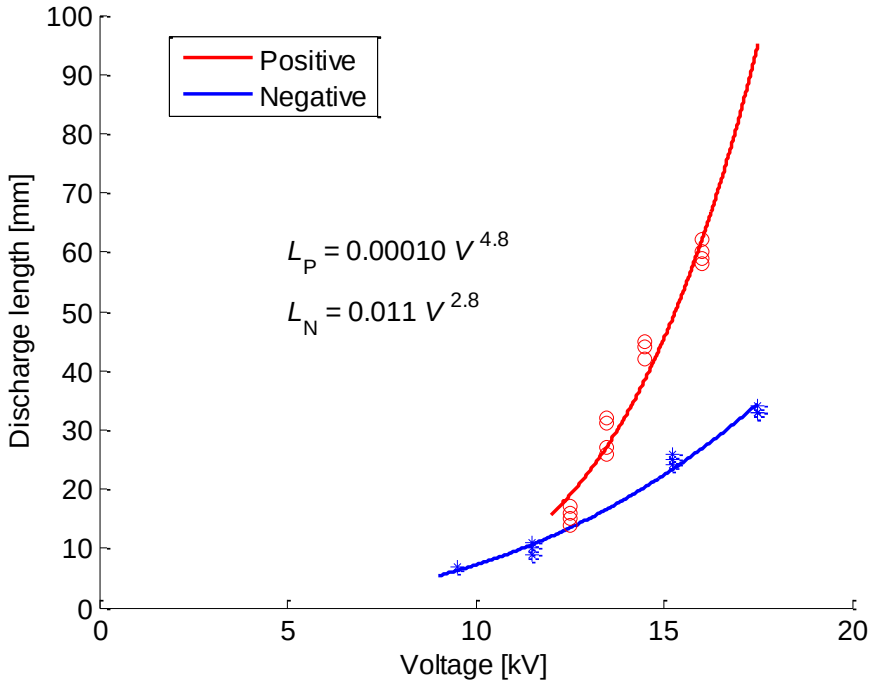

Fig. 5.1 Discharge length of surface discharge under impulse voltage application for electrodes distance d = 100 mm.

Table 5.2 Experimental condition for Fig. 5.2

Insulator	Two-layer structure pipe
Back electrode	Grounded
Distance between ring electrodes	d = 300mm
Application Voltage	Impulse

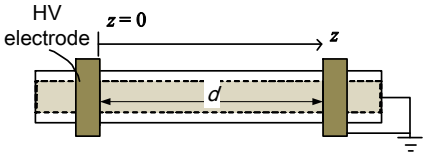

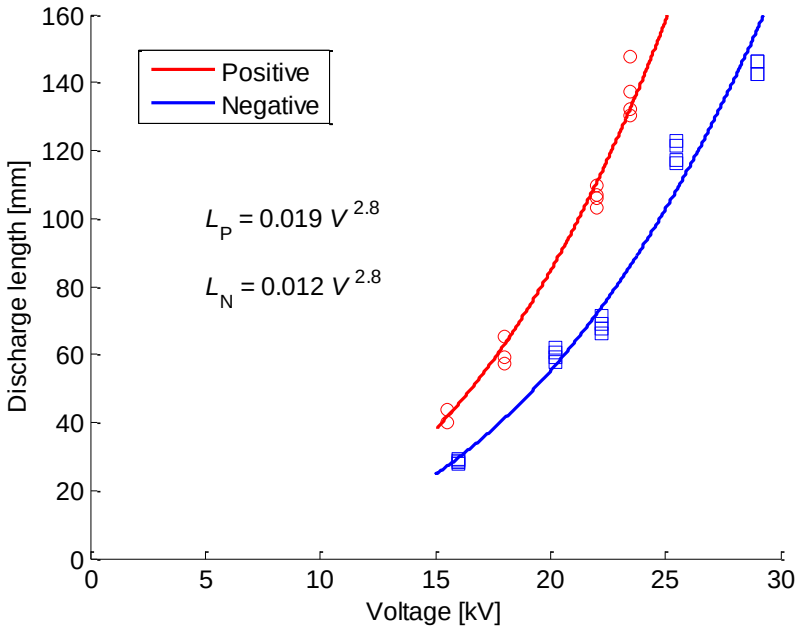

Fig. 5.2 Discharge length of surface discharge under impulse voltage application for electrodes distance d = 300 mm.

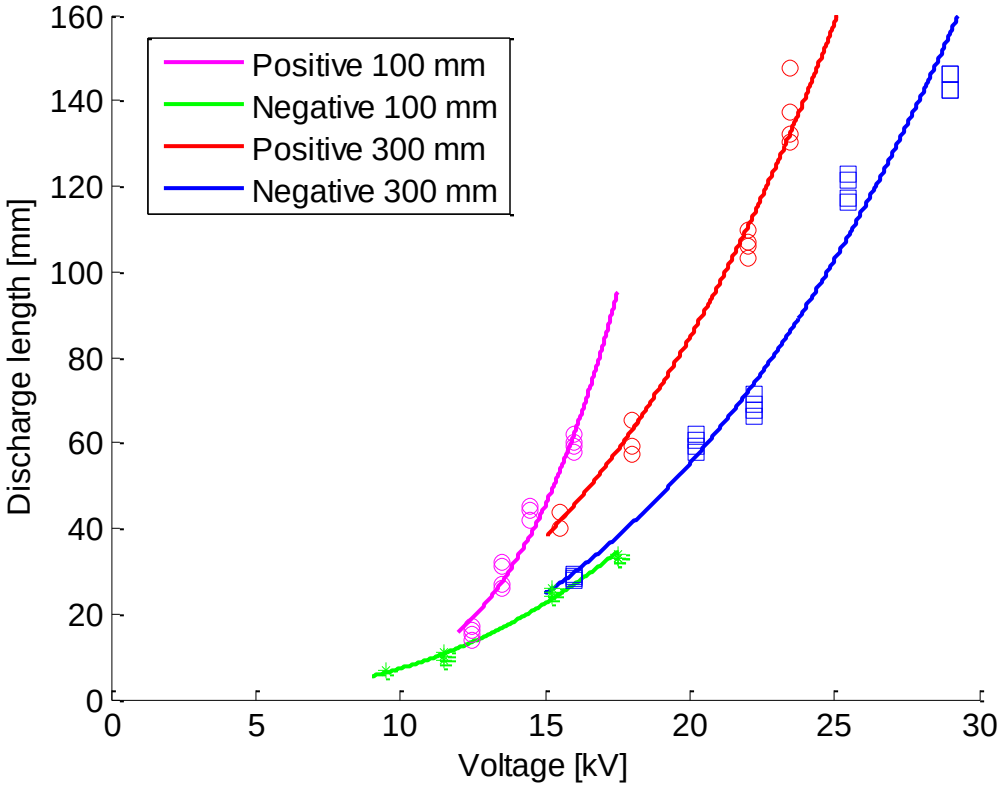

Fig. 5.3 Influence of electrodes distance on the discharge length of surface discharge

5.3 Potential and Charge Density Distributions of Positive Surface Discharge

5.3.1 Potential and residual charge distributions

Residual charge distributions of surface discharge under the application of impulse voltages are measured by the measuring system described in Section 2.4, and the potential distribution are calculated by Eq. (3.3). Figures 5.4(a), (b), (c), and (d) are respectively the potential distributions of surface discharges under 12.5 kV, 13.5 kV, 14.5 kV, and 16 kV positive impulse application voltage where the distance between the high voltage ring electrode and the grounded ring electrode is set to 100 mm.

Under the application of 12.5 kV impulse voltage, a lot of blush-like streamer discharges propagate in parallel from the high voltage electrode as shown in Fig. 5.4 (a). When 13.5kV is applied, an arborescent discharge, which corresponds to a leader discharge, propagates towards the grounded electrode through the streamer region as shown in Fig. 5.4(b). The stem of such discharge is regarded as the leader part and the filamentary discharge ahead of the leader is regarded as the streamer part.

With the increase of the application voltage, more leader discharge occurs and develops for a longer distance as shown in Figs. 5.4(c) and (d). In the suburb of the high voltage electrode, some residual charge has disappeared due to the back discharge which occurred at the tail part of the impulse voltage.

Potential profiles along surface discharges are extracted from Fig. 5.4 and are shown in Fig. 5.5 as a function of path length, L. The residual charge density profiles are also extracted and shown in Fig. 5.6. The potential in the brush-like streamer decreases almost linearly with the distance from the electrode as shown in Fig. 5.5 (a), and its gradient is 0.6 kV/mm. From Figs 5.5 (b) - (d) and 5.6 (b) – (d), it is possible to say that the potential and charge density profiles along a leader discharge can be divided into two parts: leader parts and streamer parts. The potential gradient in the streamer part increases with the application voltage and its value is from 1.0 to 1.2 kV/mm. In the leader part, it is from 0.15 kV/mm to 0.20 kV/mm and decrease with the application voltage. The dividing point of the leader and streamer is about 6 - 8 kV, which corresponds to 350 - 600 pC/mm^2. The dividing point increases with the application voltage.

Table 5.3 Experimental condition for Fig. 5. 4

Insulator	Two-layer structure pipe
Back electrode	Grounded
Distance between ring electrodes	d = 100mm
Application Voltage	Positive Impulse

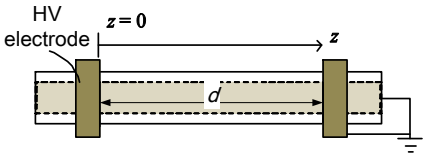

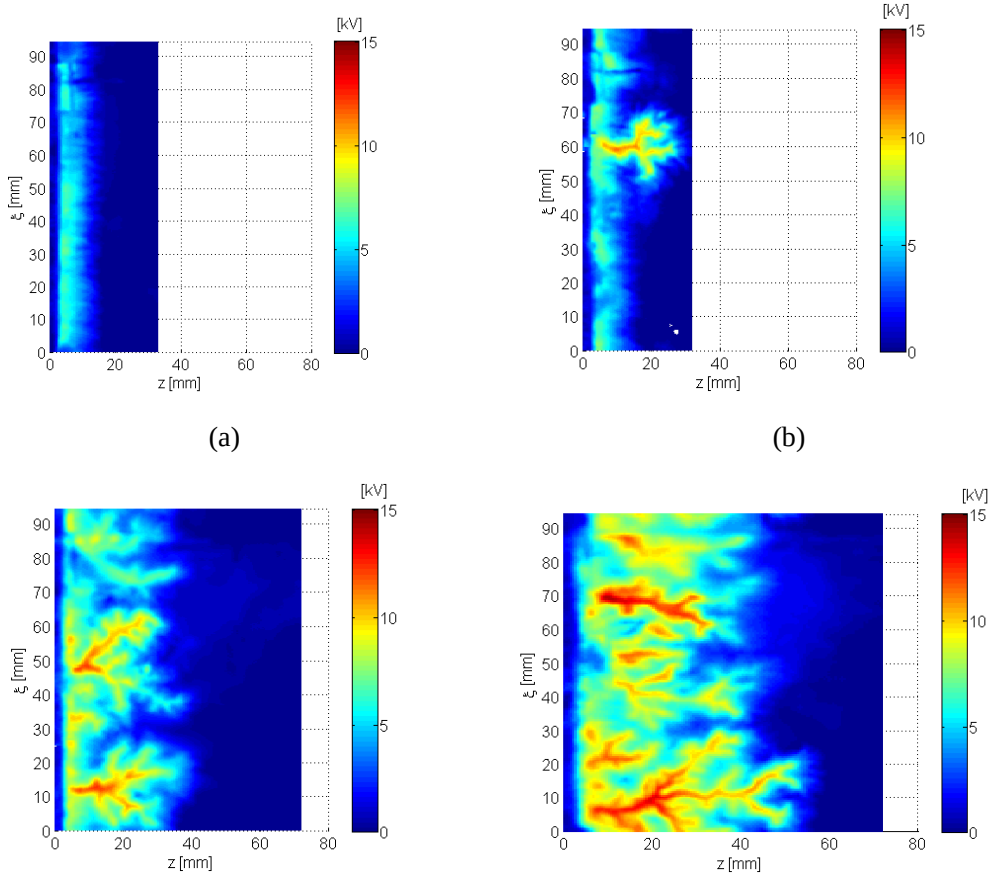

Fig. 5. 4 Potential distribution of positive surface discharge under (a) 12.5 kV, (b) 13.5 kV, (c) 14.5 kV and (d) 16 kV impulse voltage application.

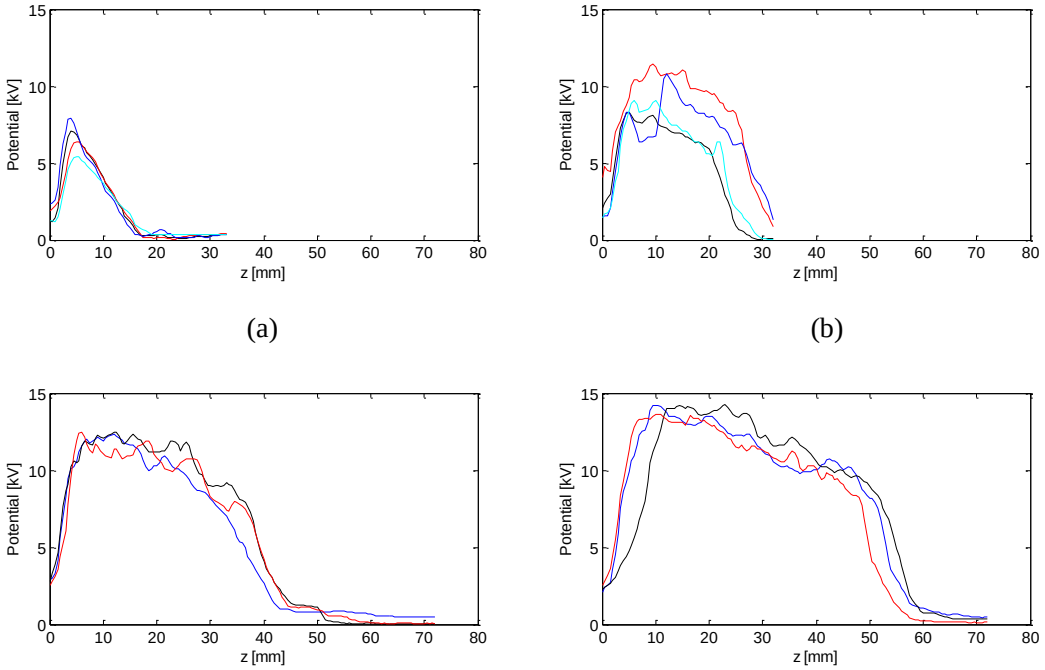

Fig. 5.5 Potential profile along surface discharge extracted from Fig. 5.5; under the application of (a) 12.5 kV, (b) 13.5 kV, (c) 14.5 kV and (d) 16 kV impulse voltage.

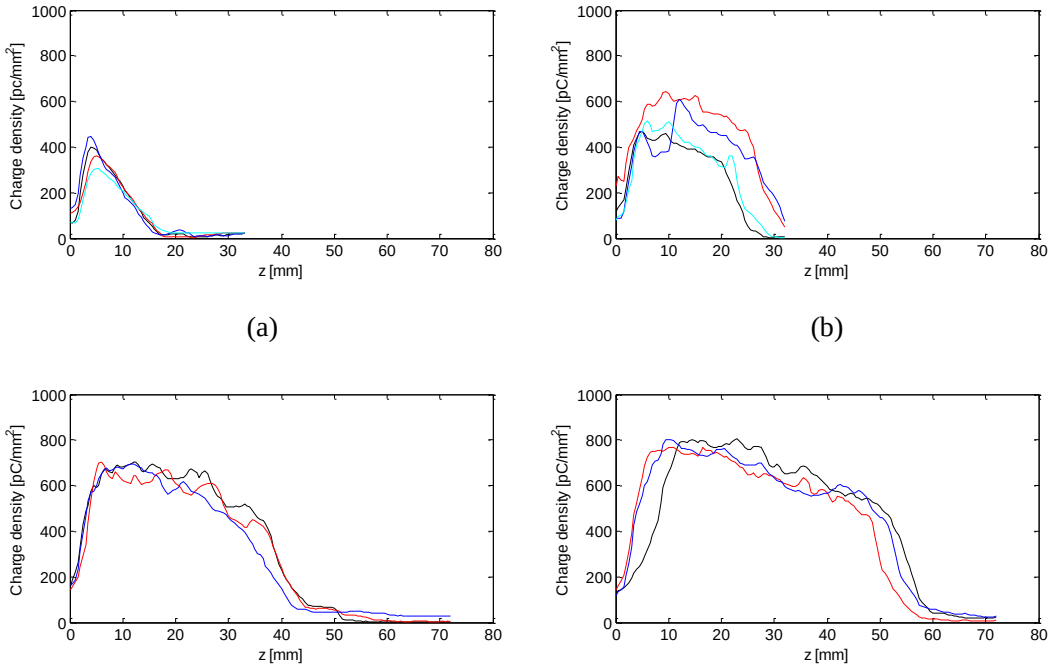

Fig. 5.6 Charge density profile along surface discharge extracted from Fig. 5.5; under the application of (a) 12.5 kV, (b) 13.5 kV, (c) 14.5 kV and (d) 16 kV impulse voltage.

5.3.2 Framing image of positive surface discharge

The framing images of propagating positive surface leader discharge under the application of 15.2 kV-impulse voltage are taken by the ultra high speed camera as shown in Fig. 5.8 with the application impulse voltage and the discharge current as shown in Fig. 5.7. The exposure time for each frame is 300 ns, and *d* is 300 mm.

The thin and luminous channel corresponds to leader channel and the luminous zone at the tip of the leader corresponds to streamer zone. The streamer zone is also referred as the ionization zone, and leader channel is of a very high conductivity where carrier can flow freely [7]. The ionization zone at the tip of the leader develops rapidly forward, and at the root of the streamer, the leader comes into being. It is to be noted that the luminous leader channel is much smaller than the radical extension of the ionization zone.

Table 5.4 Experimental condition for Fig. 5. 7 and Fig. 5. 8

Insulator	200 μm-thick PET pipe
Back electrode	Grounded
Distance between ring electrodes	d = 300mm
Application Voltage	15.2 kV, Positive Impulse

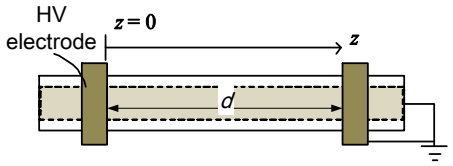

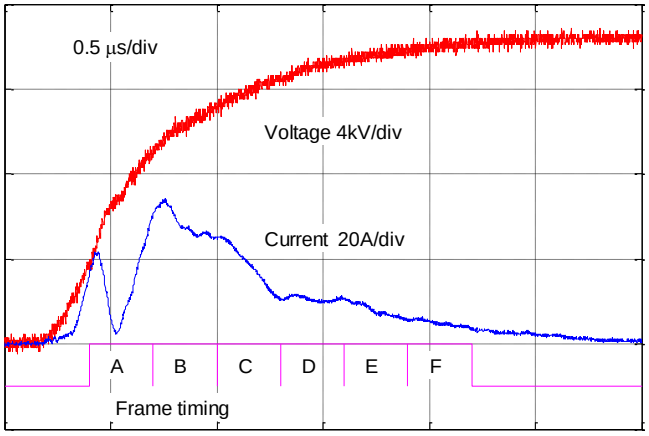

Fig. 5.7 Waveform of 15.2 kV positive impulse voltage and the discharge current.

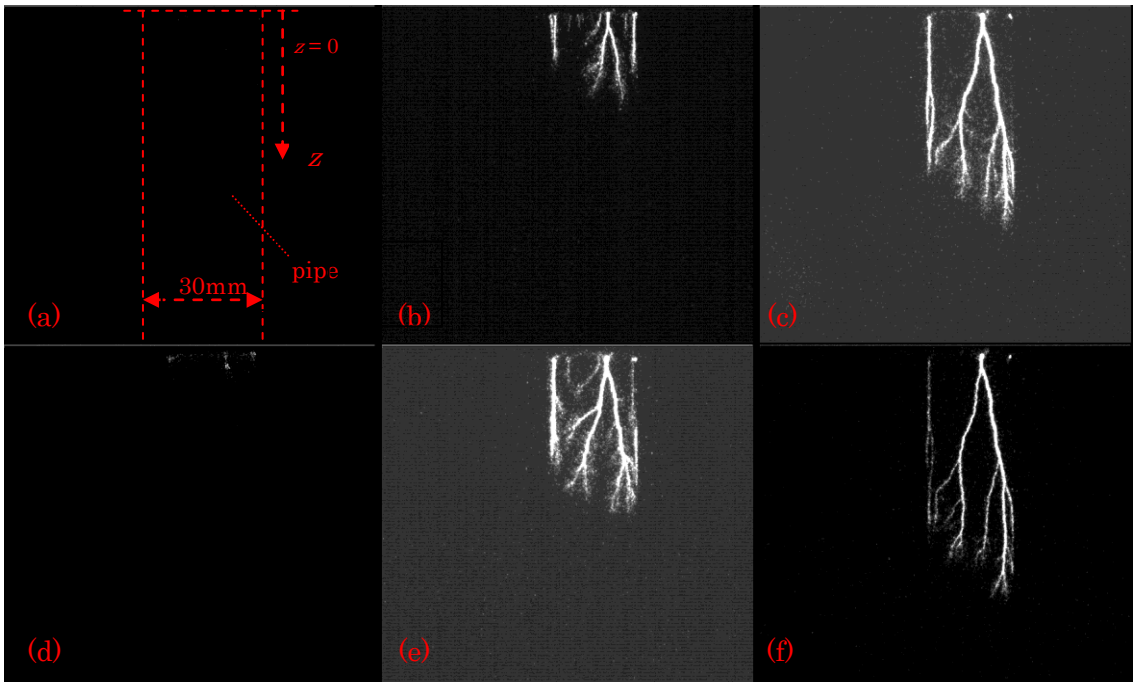

Fig. 5.8 Framing images under 15.2 kV positive impulse voltage; (a) Frame No. 1, (b) Frame No. 2, (c) Frame No. 3, (d) Frame No. 4, (e) Frame No. 5, (f) Frame No. 6.

5.3.3 Structure

In the book of M. Khalifa, the discharge in long gap is described [8] as shown in Fig. 5.9. In long gaps, if the voltage gradient at the stressed electrode exceeds the corona onset level, the ionization activity in the gap increases. As a result, a highly ionized and luminous filamentary channel, called the leader channel, develops at the electrode and propagates toward the other electrode. At the tip of the leader channel, filamentary branches called leader streamers exist where most of the ionization in the leader feed through the leader channel into the stressed electrode. Depending on the value of the instantaneous voltage gradient and the leader channel length, the leader streamer either stops after having crossed a part of the gap, or reaches the plane electrode, causing a return ionizing wave to develop there. In the latter case, the ionizing wave advances toward the leader channel tip and leads to the final jump.

In his description, the discharge includes leader channel, leader streamer, leader channel tip and streamer tip. The characteristic of “Leader” is that it is a highly ionized and luminous channel and the characteristic of “Leader streamers” is that they are filamentary branches at the tip of the leader channel. The discharge on the insulator surface is assumed to have the same structure.

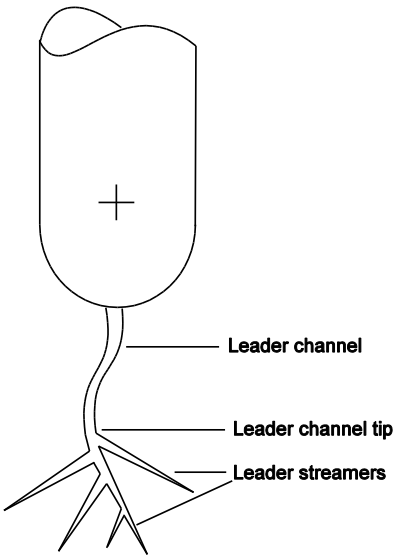

Fig. 5.9 Structure of discharge in long gap.

In this subsection, the potential distribution and field distribution under negative impulse voltage are analyzed by the method described in Chapter 3. The experimental conditions are shown in Table 5.5.

In Fig. 5.10, (a) is the waveforms , in which 1 v represents 5 kV for voltage and 1 A for current respectively, (b) is the image, (c) is the potential distribution and (d) is the electrical field distribution under 18.0 kV positive impulse application voltage. Fig.5.11 and Fig. 5.12 are respectively enlarged (a) potential distribution and (b) electrical field distribution of one front part of 18.0 kV impulse discharge in the big rectangular in Fig.5.10.

In Fig. 5.14, (a) shows the waveforms , in which 1 v represents 5 kV for voltage and 1 A for current respectively), (b) shows the image, (c) shows the potential distribution and (d) shows the electrical field distribution under 23.5 kV positive impulse application voltage. Fig. 5.15 shows the enlarged (a) potential distribution and (b) electrical field distribution of 23.5 kV impulse discharge in the big rectangular in Fig.5.17. Fig. 5.16 shows the enlarged (a) potential distribution and (b) potential along across-direction and (c) potential along longitude-direction of 23.5 kV impulse discharge in the small rectangular in Fig.5.14(c). Fig. 5.16 shows the enlarged (a) electrical field distribution and (b) electrical field along across-direction and (c) electrical field along longitude-direction of 23.5 kV impulse discharge in the small rectangular in Fig.5.17(d).

From Figures 5.10 ~ 5.17, it shows that the structure of surface discharge under positive impulse has the same structure of the discharge in long gaps. That is, it includes leader channel, leader streamer, leader channel tip and streamer tip.

In the leader channel, it is highly ionized, and the potential is very high, the potential gradient is low and the field is low. In the streamer channel, the potential gradient is higher and the field is higher than those in the leader channel. At the leader channel tip, the field is as high as to 2 kV/mm and at the streamer tip, the field is as high as to 1 kV/mm. Because the size of the streamer tip is much smaller than the probe sensor, the spatial resolution is not good enough to measure the streamer tip, the field should be much higher than 1 kV/mm.

Table 5.5 Experimental condition for section 5.4

Insulator	Two-layer structure pipe
Back electrode	Grounded
Distance between ring electrodes	d = 300mm
Application Voltage	Positive Impulse

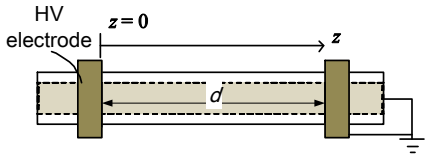

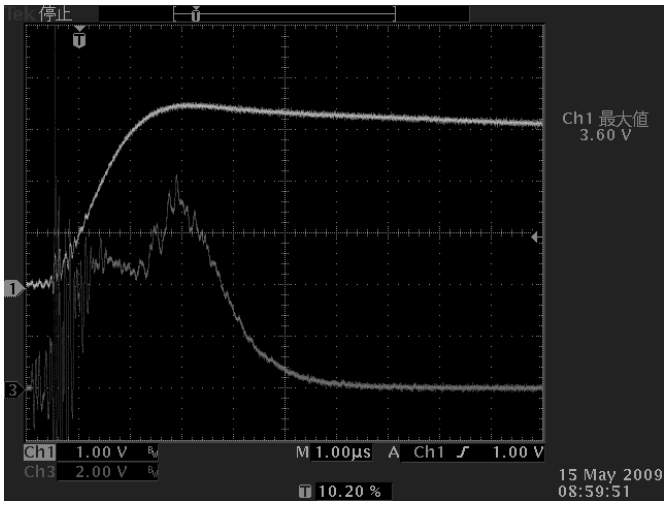
停止
Ch1 最大値
3.60 V
Ch1 1.00 V
Ch3 2.00 V
M 1.00µs A Ch1 1.00 V
10.20 %
15 May 2009
08:59:51

(a)

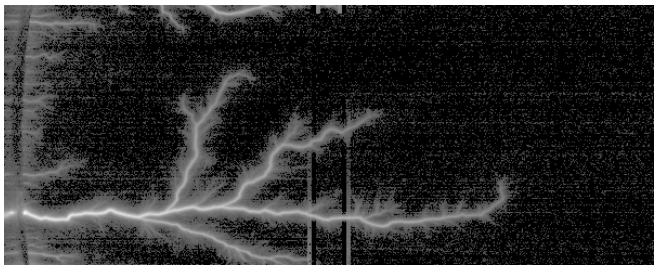

(b)

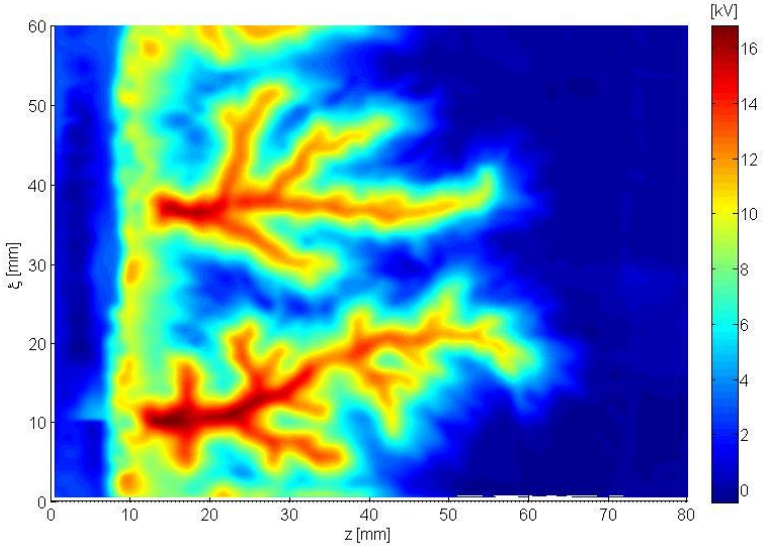
[kV]
16
14
12
10
8
6
4
2
0
60
50
40
30
20
10
0
ξ [mm]
0
10
20
30
40
50
60
70
80
z [mm]

(c)

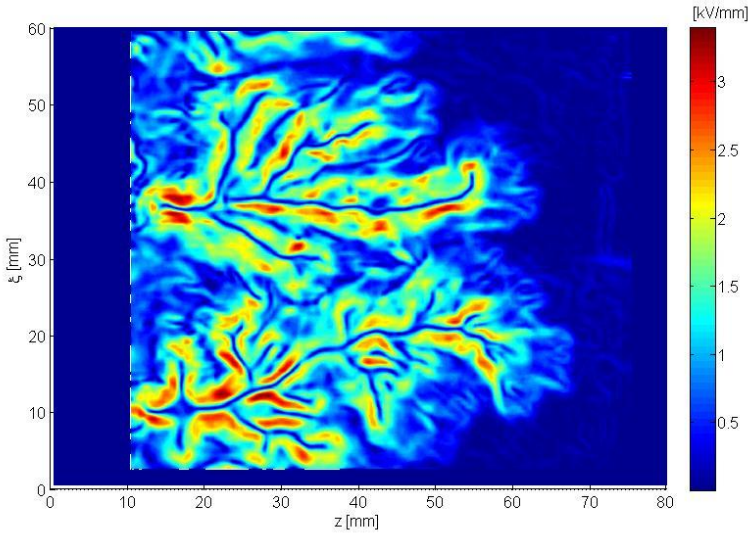

(d)

Fig.5.10 (a) waveforms (1 v represents 5 kV for voltage and 1 A for current respectively), (b) image, (c) potential distribution and (d) electrical field distribution under 18.0 kV positive impulse application voltage.

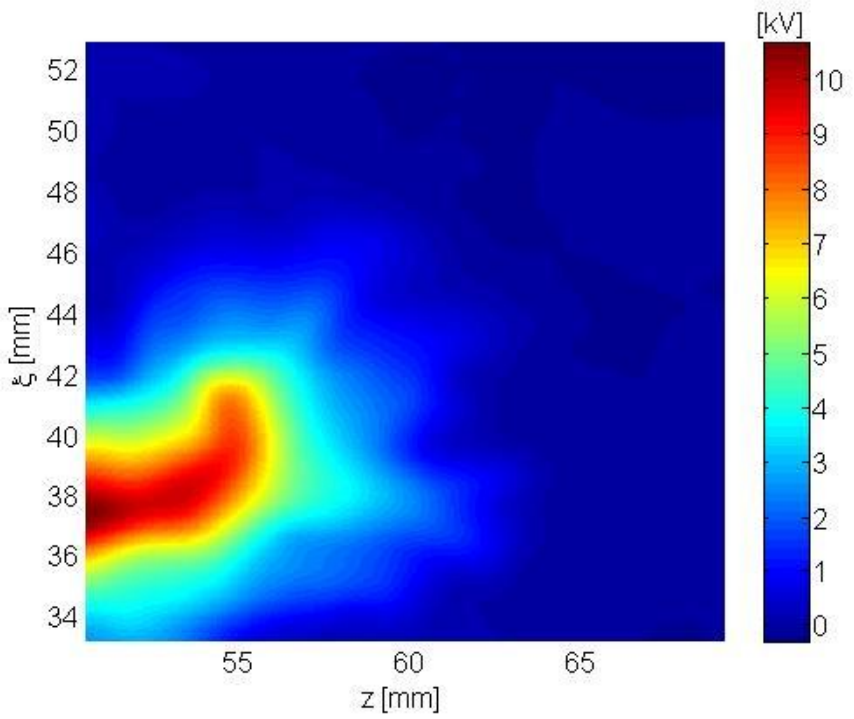

(a)

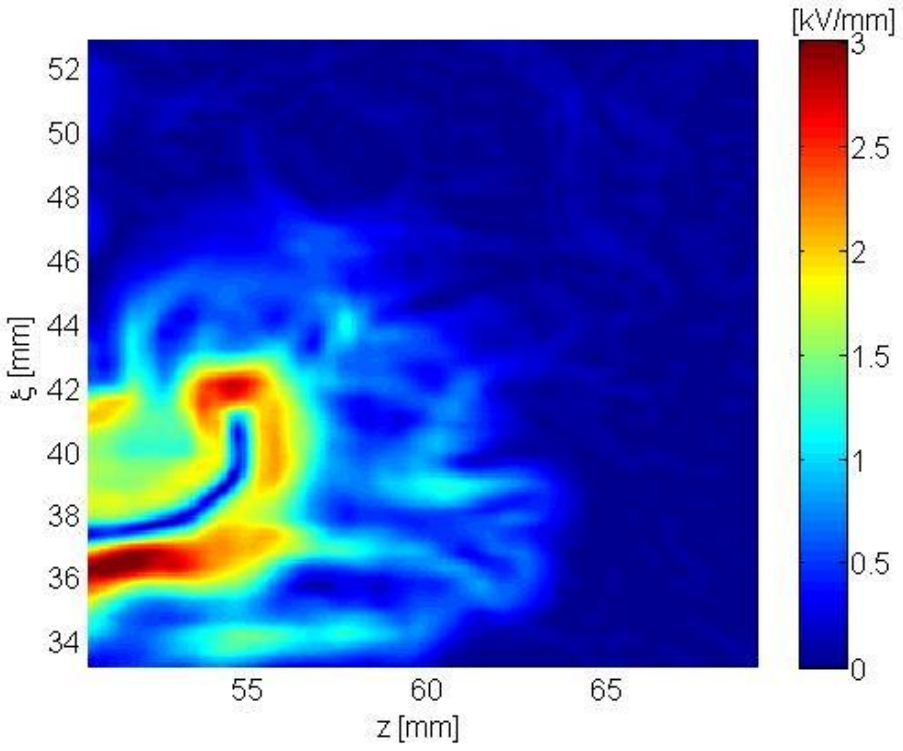

(b)

Fig.5.11 Enlarged (a) potential distribution and (b) electrical field distribution of 18.0 kV impulse discharge of a front part in Fig.5.10.

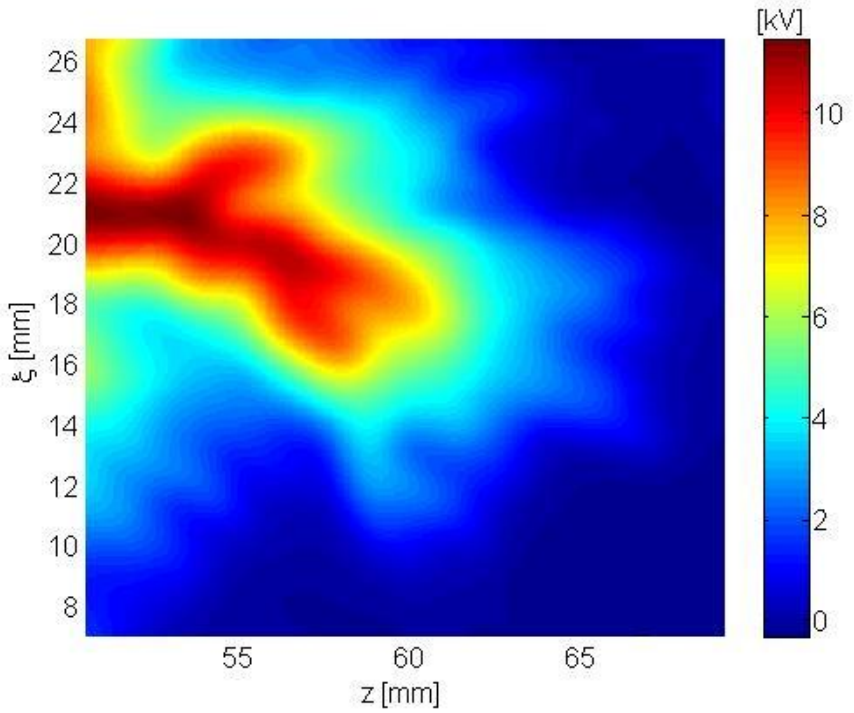

(a)

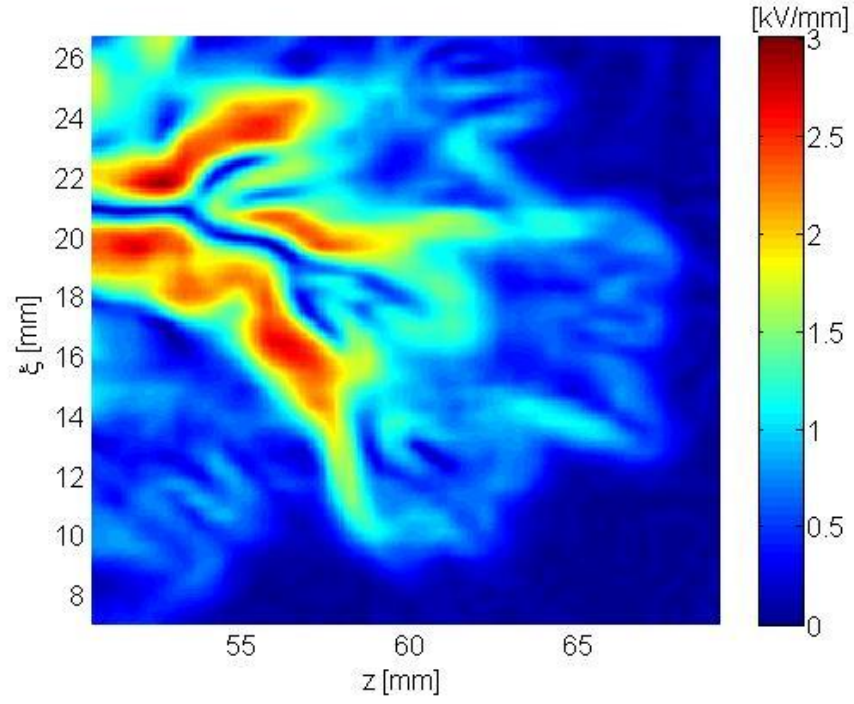

(b)

Fig.5.12 Enlarged (a) potential distribution and (b) electrical field distribution of 18.0 kV impulse discharge of a front part in Fig.5.10.

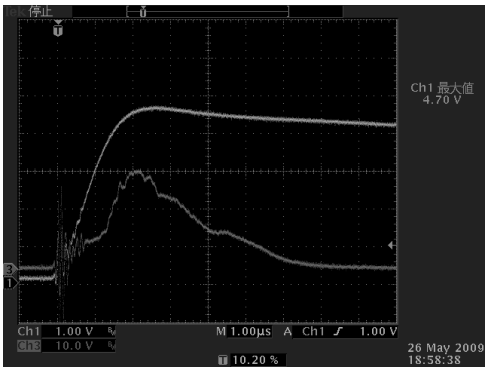

(a)

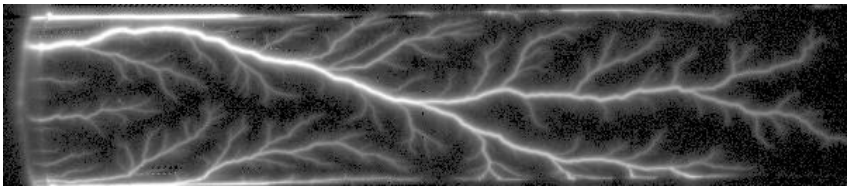

(b)

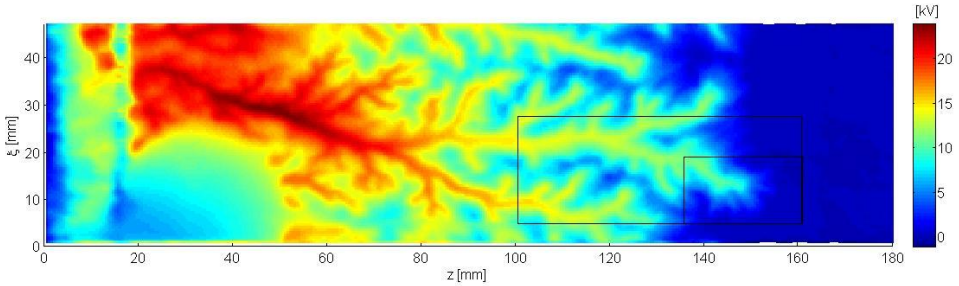

(c)

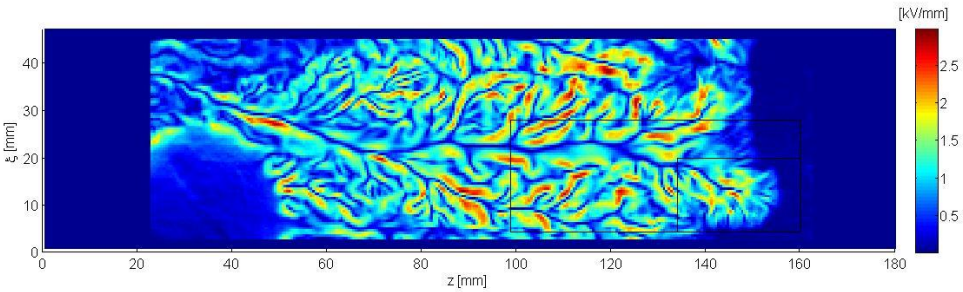

(d)

Fig.5.13 (a) waveforms (1 v represents 5 kV for voltage and 1 A for current respectively), (b) image, (c) potential distribution and (d) electrical field distribution under 23.5 kV positive impulse application voltage.

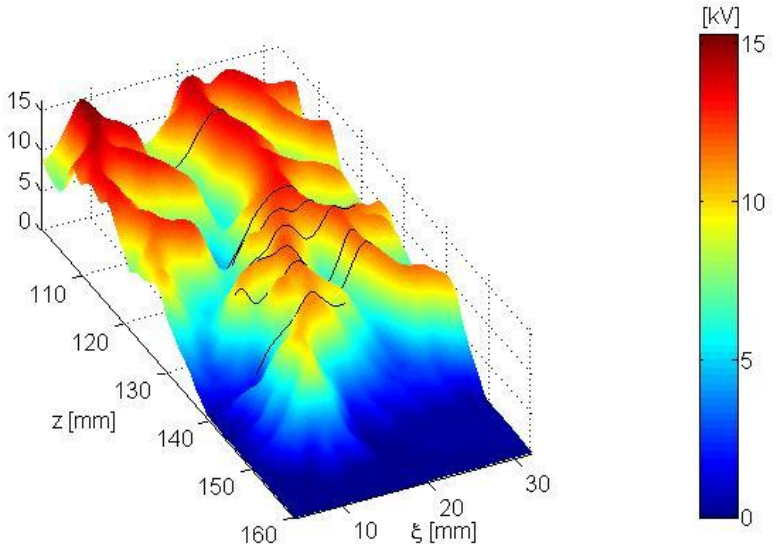

(a)

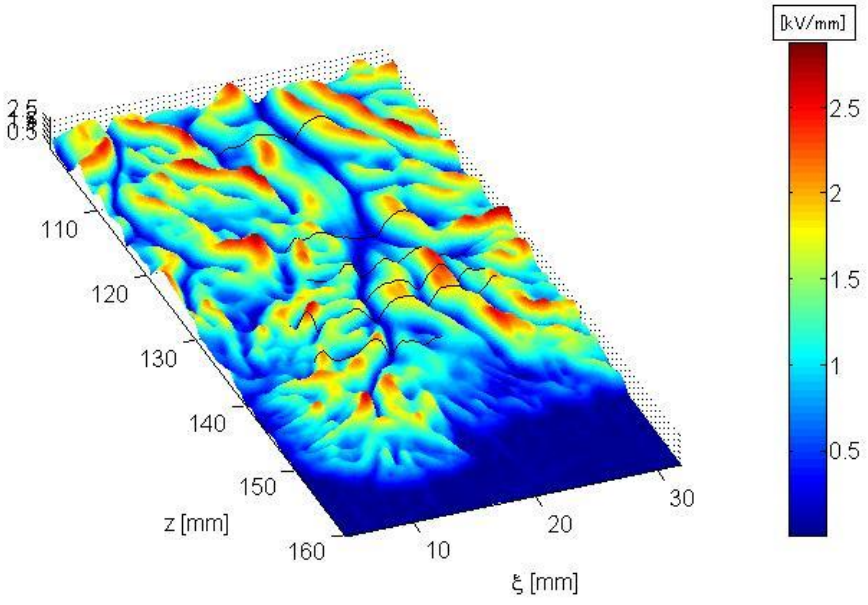

(b)

Fig.5.14 Enlarged (a) potential distribution and (b) electrical field distribution of 23.5 kV impulse discharge in the big rectangular in Fig.5.17.

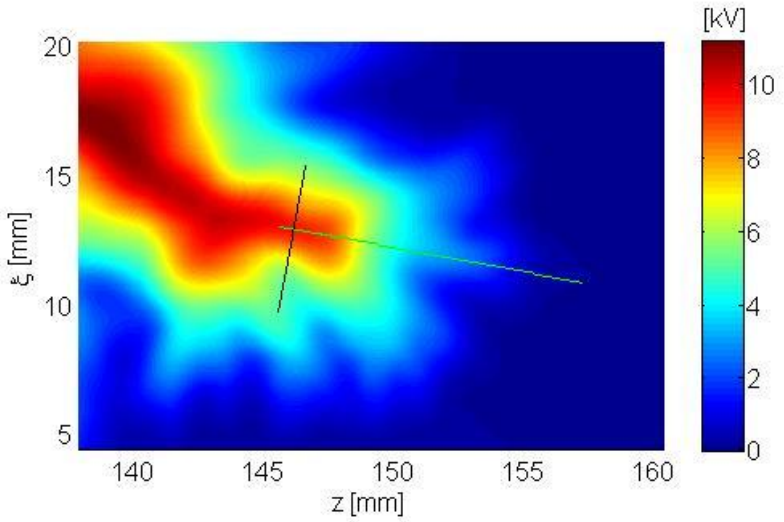

(a)

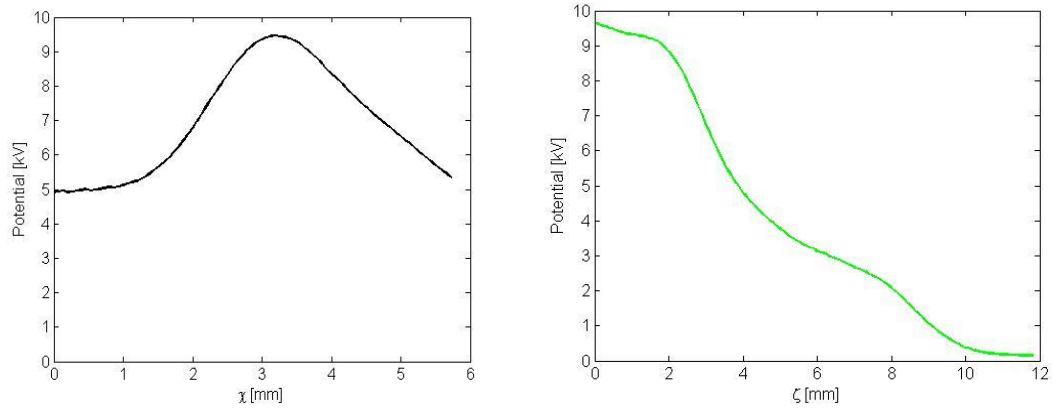

(a) (c)

Fig.5.15 Enlarged (a) potential distribution and (b) potential along across-direction and (c) potential along longitude-direction of 23.5 kV impulse discharge in the small rectangular in Fig.5.17(c).

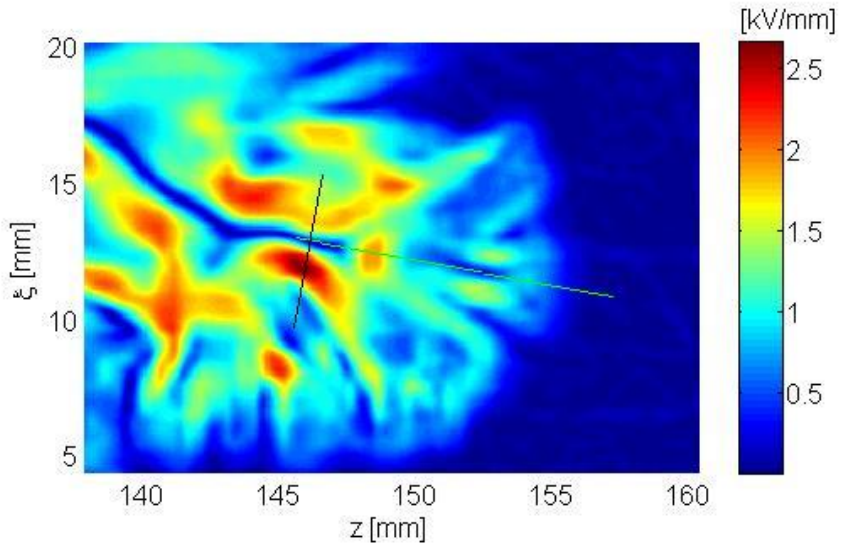

(a)

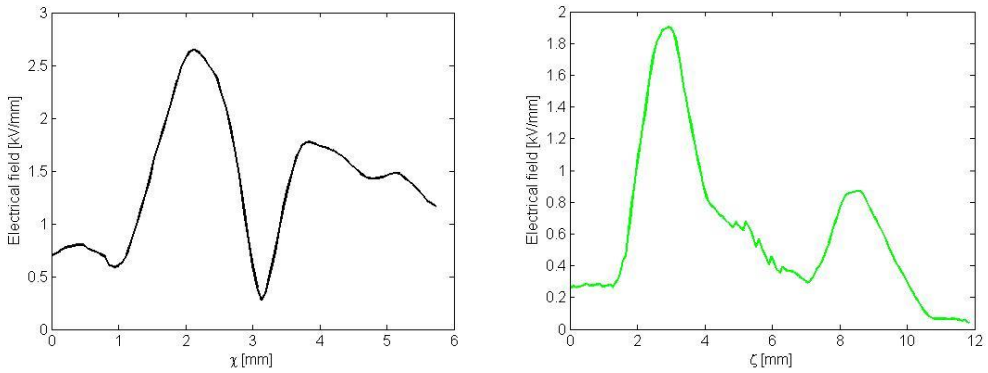

(b) (c)

Fig.5.16 Enlarged (a) electrical field distribution and (b) electrical field along across-direction and (c) electrical field along longitude-direction of 23.5 kV impulse discharge in the small rectangular in Fig.5.17(d).

5.4 Potential and Charge Density Distributions of Negative Surface Discharge

5.4.1 Potential and residual charge distributions

In the same manner, the potential and charge density distributions of negative surface discharges are measured for d = 100 mm, and 300mm, with changing the application voltage. Figures 5.17, 5.18 and 5.19 show respectively the potential distribution, the potential profiles along negative surface discharges, and the charge density distribution for d = 100 mm.

Under the application of -9.5kV impulse voltage, a lot of blush-like streamer discharges propagate in parallel from the high voltage electrode as shown in Fig. 5.17(a). With increasing application voltage, leader discharges are formed and propagate for longer length in parallel with each other without branching.

The potential in the brush-like streamer decreases with the distance from the electrode as shown in Fig. 5. 18 (a) and (b), and its gradient takes its peak on the head part of the streamer and is 1.5 kV/mm. From Figs 5.18 (c) - (d) and 5.19 (d) - (d), the potential and charge density profiles along a leader discharge can be divided into two parts as well as a positive leader discharge: leader parts and streamer parts. The averaged potential gradient in the negative streamer part is from 1.0 kV/mm to 1.6 kV/mm, and in the leader part, it is from 0.15 kV/mm to 0.20 kV/mm. The dividing point of the leader and streamer is 8 - 10 kV which corresponds to 500 - 600 pC/mm^2.

Table 5.6 Experimental condition for Fig. 5.17 - 5.19.

Insulator	Two-layer structure pipe
Back electrode	Grounded
Distance between ring electrodes	d = 100mm
Application Voltage	Positive Impulse

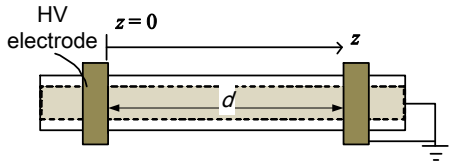

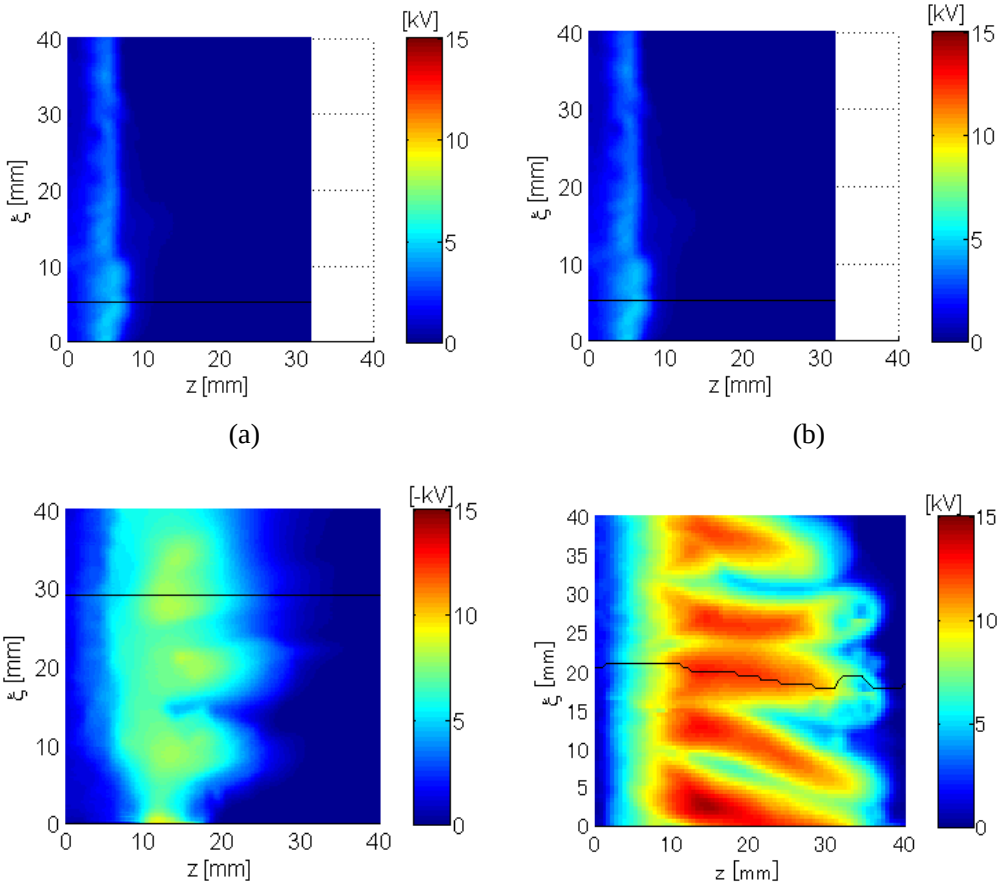

Fig. 5.17 Potential distribution under (a) -9.5 kV, (b) -11.5 kV, (c) -15.25 kV and (d) -17.5 kV impulse voltage application.

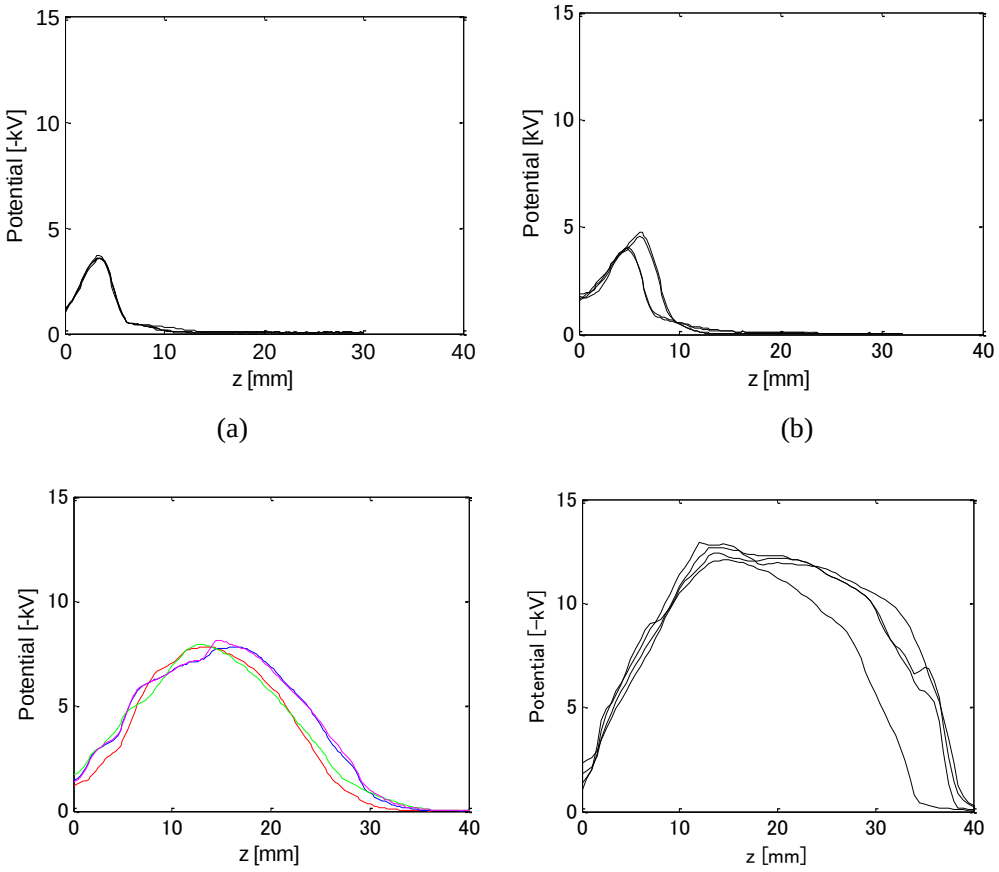

Fig. 5.18 Potential along z-direction under (a) -9.5 kV, (b) -11.5 kV, (c) -15.25 kV and (d) -17.5 kV negative impulse voltage application.

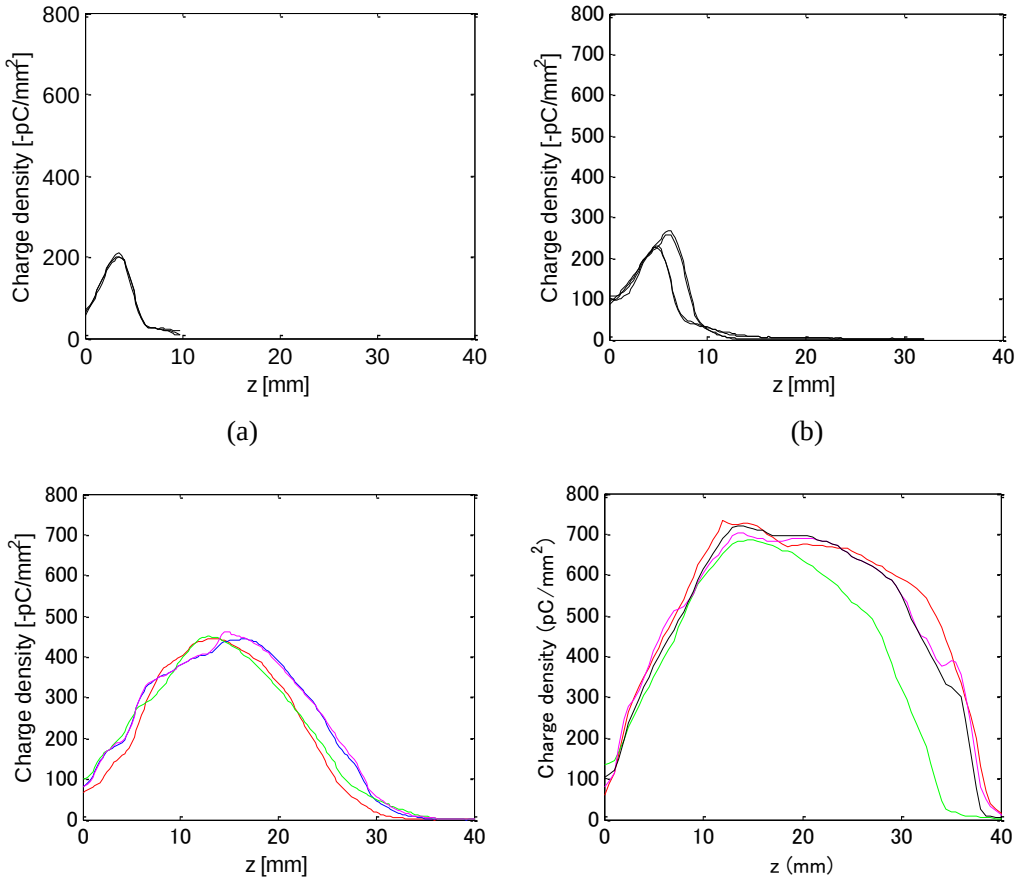

Fig. 5.19 Potential along z-direction under (a) -9.5 kV, (b) -11.5 kV, (c) -15.25 kV and (d) -17.5 kV negative impulse voltage application.

5.4.2 Framing Image

The framing images of propagating positive surface leader discharge under the application of -15.2 kV-impulse voltage are taken by the ultra high speed camera as shown in Fig. 5.20 with the application impulse voltage and the discharge current as shown in Fig. 5.19. The exposure time for each frame is 300 ns, and *d* is 300 mm. The experimental conditions are shown in Table 5.7.

As well as positive leader discharge, the luminous thin channels and the luminous zones ahead of them, which correspond to the leader channels and streamer zone, respectively, are recognized.

Table 5.7 Experimental condition for Fig. 5. 7 and Fig. 5. 8

Insulator	200 μm-thick PET pipe
Back electrode	Grounded
Distance between ring electrodes	d = 300mm
Application Voltage	-15.2 kV, Negative impulse

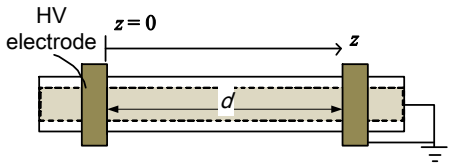

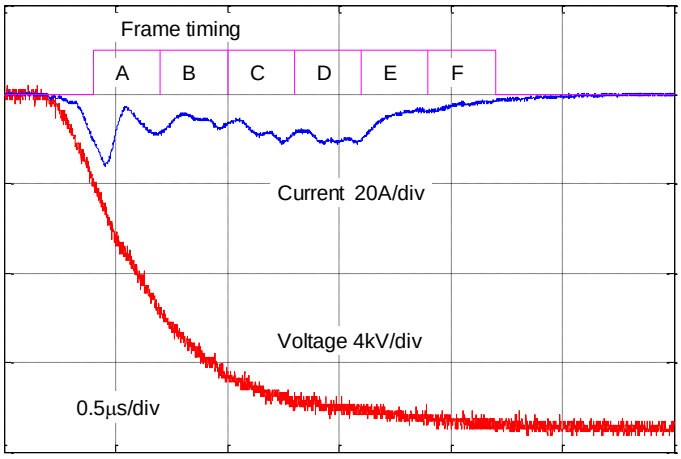

Fig. 5.20 Waveform of -15.2 kV negative impulse voltage and the discharge current.

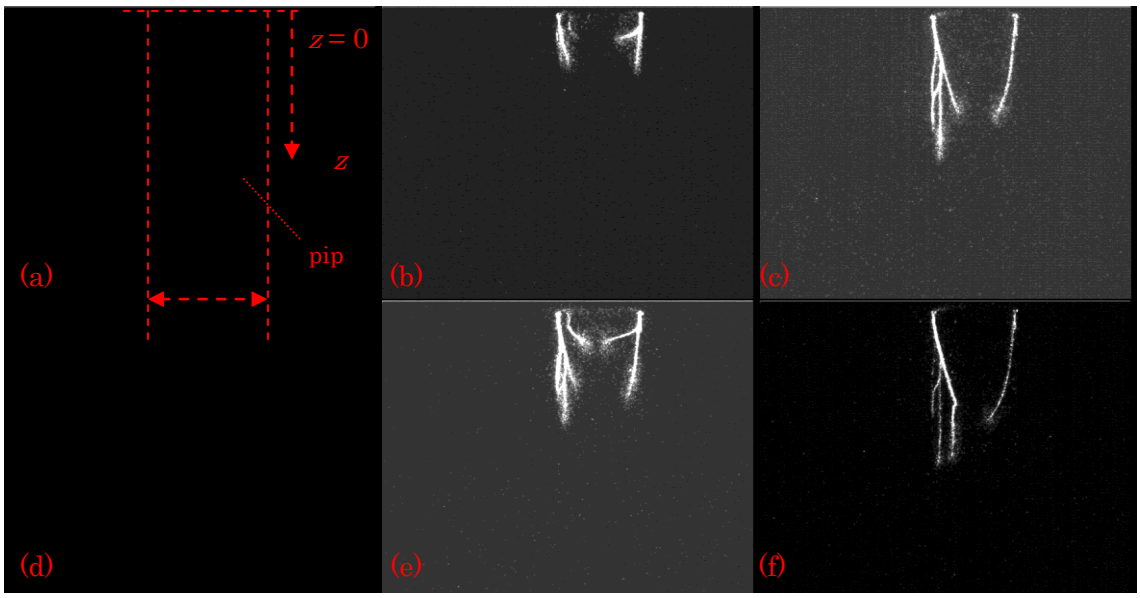

Fig. 5.21 Framing images under -15.2 kV impulse voltage; (a) Frame No. 1, (b) Frame No. 2, (c) Frame No. 3, (d) Frame No. 4, (e) Frame No. 5, (f) Frame No. 6.

5.4.3 Structure

As well as the positive discharge, the electric field distribution around negative surface discharge is calculated from the measured potential distribution by the method described in chapter 3. Figure 5.22 shows potential and electrical field distribution on pipe insulator under the application of -15.25 kV impulse voltage: Fig. 5.22(a) shows potential, (b) shows the horizontal component intensity of the electrical field, $|E_h|$ (c) shows the perpendicular component intensity of the electrical field, $|E_v|$, and (d) shows the electrical field intensity, $|E|$. Since the PET film is very thin, there is little difference among the distribution-patterns of the potential, the perpendicular component intensity of the electrical field and the total intensity of the electrical field.

The horizontal component of the electrical field is the determining factor of surface discharge propagation, therefore, only the potential distribution and the horizontal component of the electrical field are discussed here.

The potential profiles along and across the discharge, which corresponds to those along black and red line, respectively, are extracted as shown in Fig. 5.23. In the same manner, the profiles of electrical field $|E_h|$ along and across the discharge are extracted as shown in Fig. 5.22. In the center of the discharge, there is a thin channel with a low electrical field corresponding to the leader channel. On the periphery of this ionization zone, the electrical field is high and it reaches 1.2 kV/mm.

In Fig.5.25, (a) is waveforms, in which 1 v represents 5 kV for voltage and 1 A for current respectively, (b) is the image corresponding to the range in the black-box in (c) and (d) , (c) is the potential distribution and (d) is the electrical field distribution of -22.25 kV negative impulse discharge. In Fig.5.26, (a) is the potential distribution and (b) is the potential along the longitude-direction of -22.25 kV negative impulse discharge. In Fig. 5.27, (a) is the electrical field distribution and (b) is the electrical field along the longitude-direction of -22.25 kV negative impulse discharge.

From the above figures, it is found that the in the channel of the leader, the electrical field is very low and the conductivity is very high. At the periphery of the streamer zone, the electrical field is very high.

It is supposed that the negative discharge also includes leader channel, leader tip, streamer and streamer tip just as positive discharge, but the positive streamers are many very thin and short channels and can not be distinguished by the probe. The leader tip is very near to the streamer tip.

Table 5.8 Experimental condition for section 5.4

Insulator	Two-layer structure pipe
Back electrode	Grounded
Distance between ring electrodes	d = 300mm
Application Voltage	Neagtive Impulse

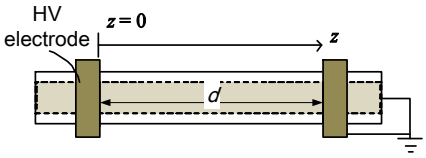

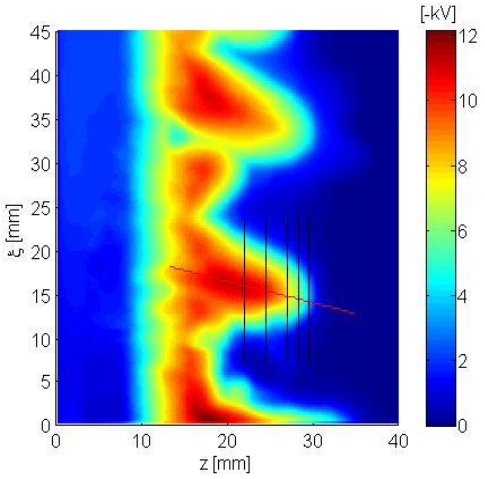

(b)

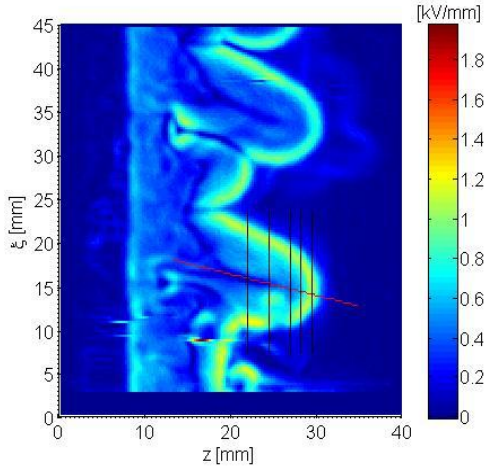

(b)

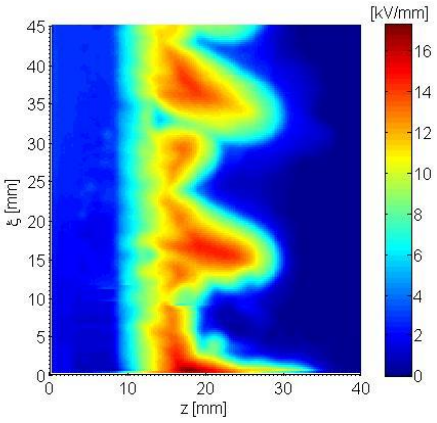

(c)

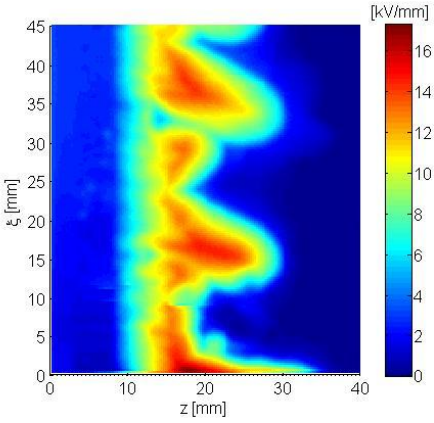

(d)

Fig. 5.22 (a) potential distribution, (b) horizontal component of the electrical field, (c) perpendicular component of the electrical field, (d) the electrical field distribution under -15.25 kV impulse application voltage.

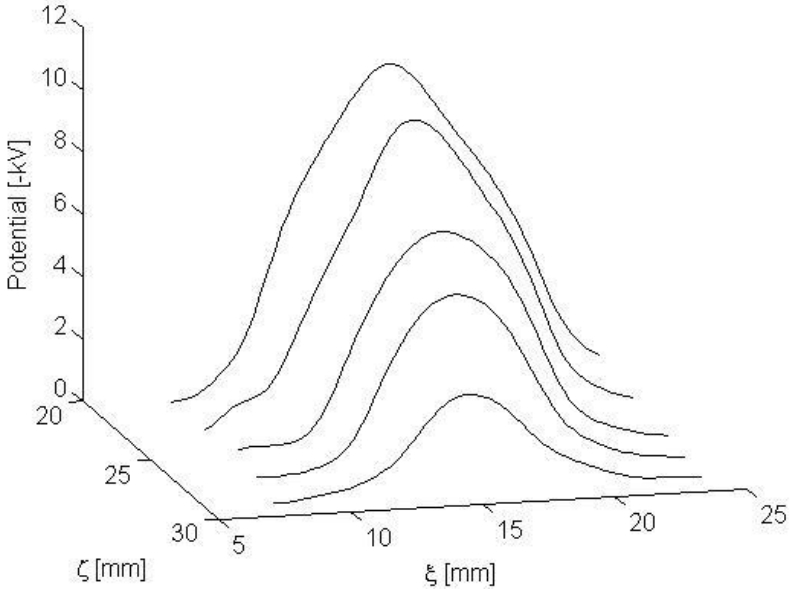

(a)

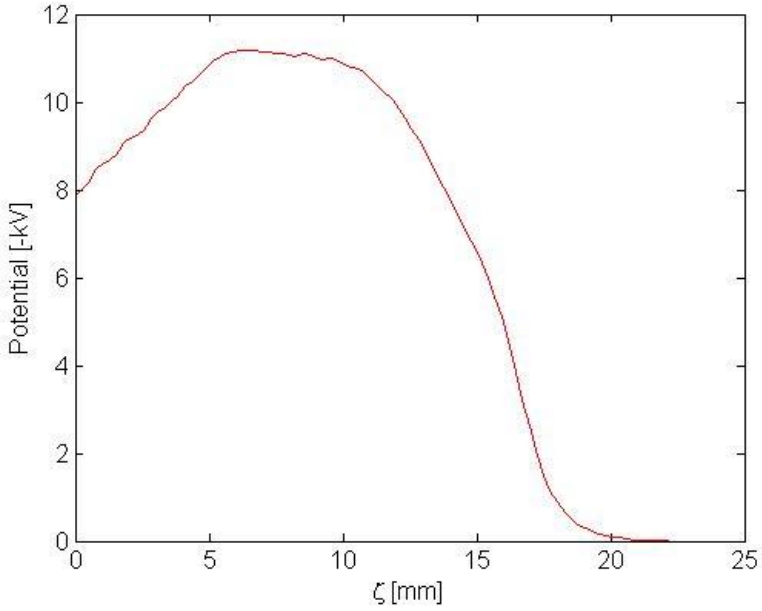

(b)

Fig. 5.23 Potential distribution along (a) the black line and (b) the red line in Fig. 5.22(a).

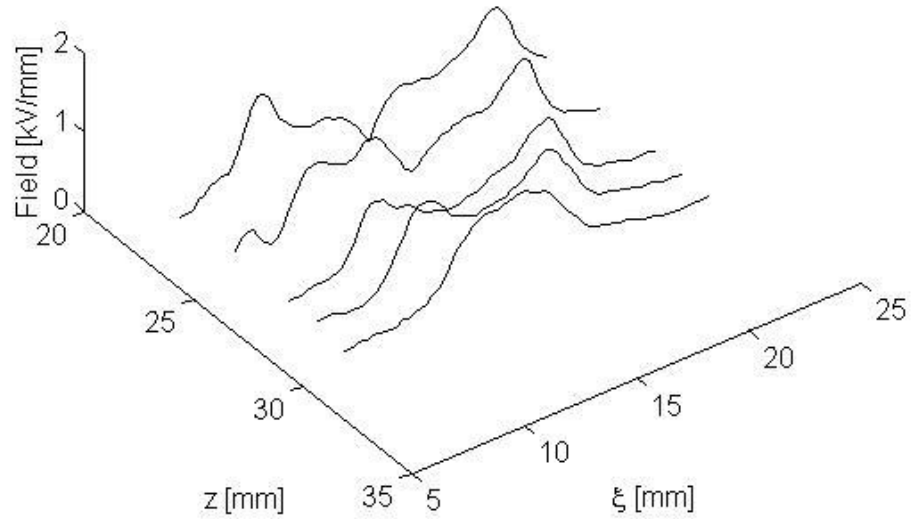

(a)

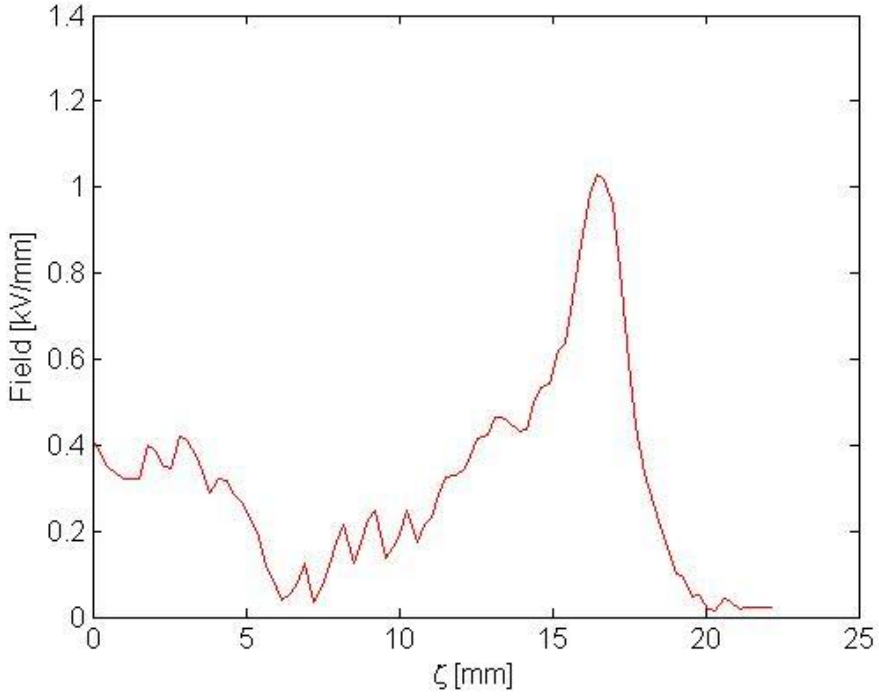

(b)

Fig.5.24 Electrical field distribution along (a) the black line and (b) the red line in Fig.5.7(b).

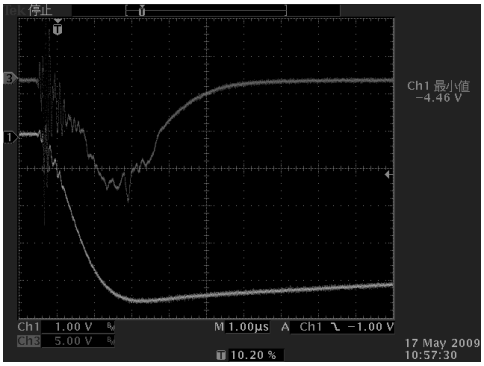

(a)

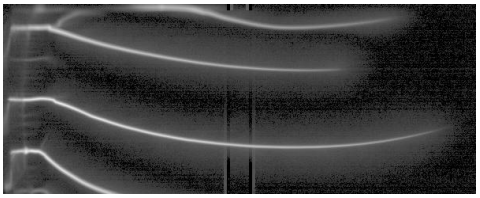

(b)

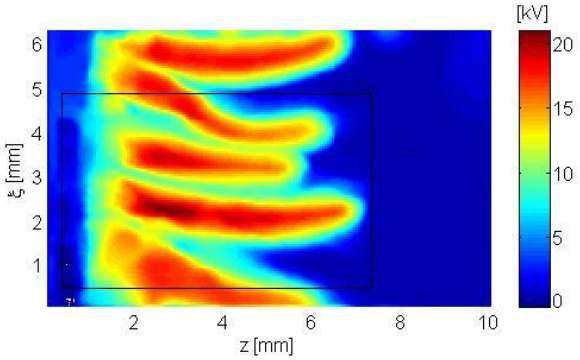

(c)

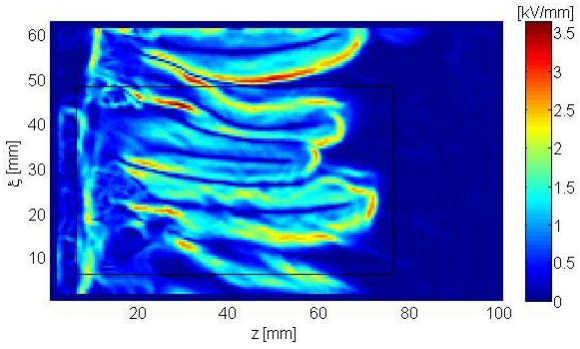

(d)

Fig.5.25 (a) waveforms (1 v represents 5 kV for voltage and 1 A for current respectively), (b) image, (c) potential distribution and (d) electrical field distribution of -22.25 kV negative impulse discharge.

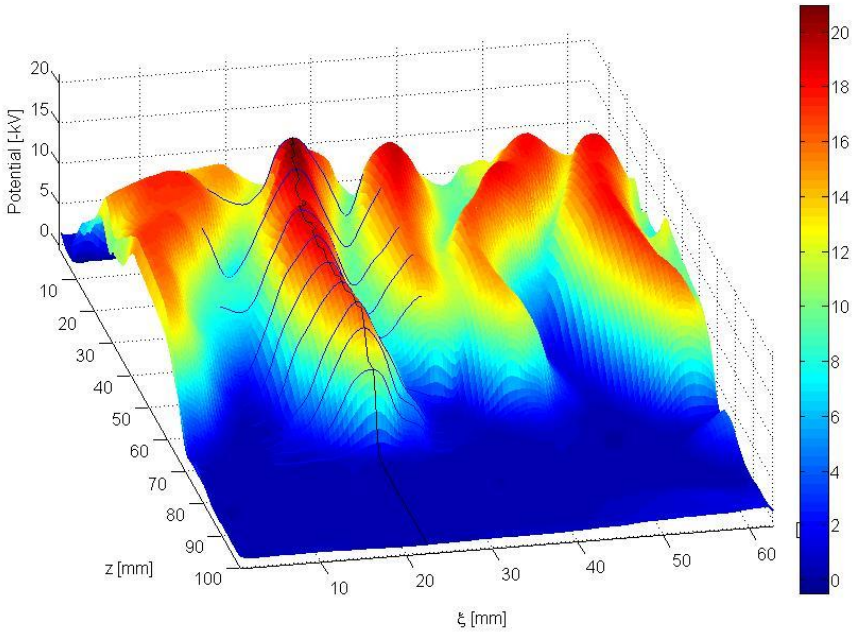

(a)

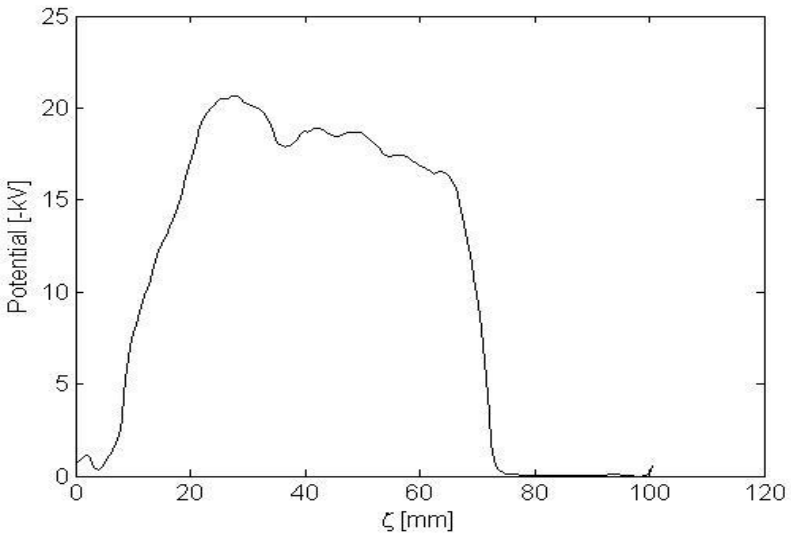

(b)

Fig.5.26 (a) potential distribution and (b) potential along the longitude-direction of -22.25 kV negative impulse discharge.

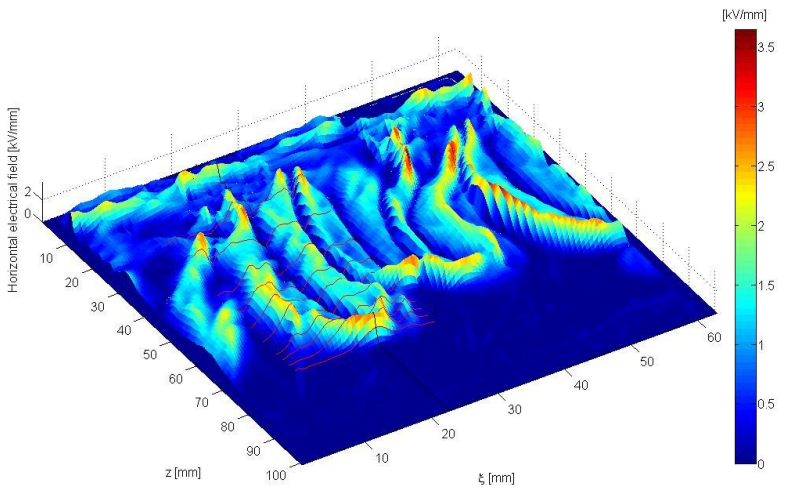

(a)

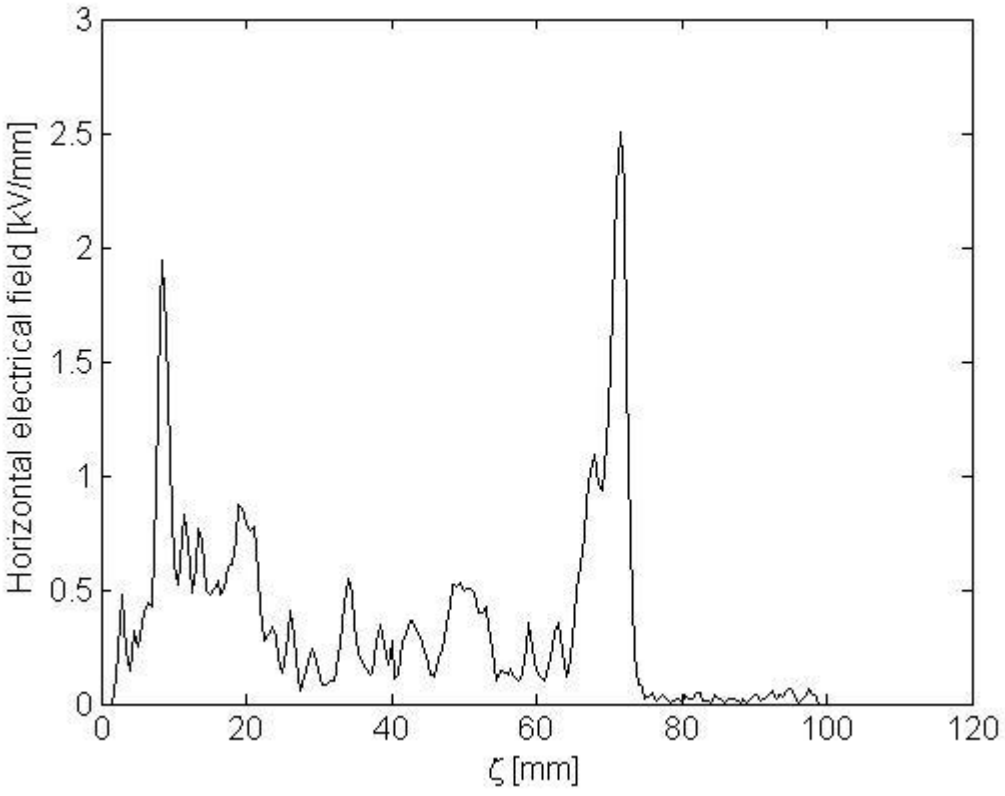

(b)

Fig.5.27 (a) electrical field distribution and (b) electrical field along the longitude-direction of -22.25 kV negative impulse discharge.

5.5 Summary

In this chapter, the propagation characteristics of surface discharge under impulse application voltage are studied.

a) The function between the discharge length and the application voltage is gotten, the discharge length under positive discharge is longer than that under negative impulse voltage.
b) The potential gradient in the leader part and streamer part is gotten.
c) It is found that in the channel of the leader, the electrical field is very low and the conductivity is very high. At the periphery of the streamer zone, the electrical field is very high.

Reference

[1] L. Niemeyer and F. Pinnekamp. "Leader Discharge in SF6". *J.Phys. D: Appl. Phys.*, Vol. 16, pp. 1031-1045, 1983.

[2] L. Niemeyer, L. Ullrich and N. Wiegart. "The Mechanism of Leader Breakdown in Electronegative Gases". IEEE Trans. On Electrical Insulation, Vol. 24, pp. 309-324, 1989.

[3] Q. Zhang, L. Yang, Q. Chen, M Hara and Y. Qiu. "The Effect of Impulse Rising Steepness on Streamer to Leader Transition in Non-uniform Field Gap in SF6". *J.Phys. D: Appl. Phys.*, Vol. 36, pp. 1212-1216, 2003.

[4] O. Yamamoto, T. Hara and T. Takuma. "The Role of Leader Re-illumination in the development of Surface Discahrge in SF6 Exposed to a Very Fast Transient Overvoltage". *J.Phys. D: Appl. Phys.*, Vol. 31, pp. 2997-3003, 1998.

[5] Y. Qiu, W. Gu, Q. Zhang and E. Kuffel. "The pressure Dependence of the Leader Stepping Time for a Positive Point-plane Gap in SF6 Gas". *J.Phys. D: Appl. Phys.*, Vol. 31, pp. 3252-3254,1998.

[6] A. Kupershtokh, V. Charalambakos, D. Agoris and D. Karpov. "Simulation of breakdown in air Using Cellular Automata with Streamer to Leader Transition". *J.Phys. D: Appl. Phys.*, Vol. 34, pp. 936-946, 2001.

[7] L. Niemyer and F. Pinnekamp, "Leader discharge in SF6", *J. Phys. D: Appl. Phys*, Vol.16, 1983, pp. 1031-1045.

[8] M. Khalifa, *High-Voltage Engineering*, Gina, Egypt, New York and Basel, 1990.

Chapter 6

The Influence of Residual Charge on Surface Discharge Propagation

6.1 Introduction

For the high voltage electrical apparatus, the operating conditions are very complex and have to withstand all kinds of overvoltage, including VFTO (very fast transient overvoltage), lightning overvoltage, switching overvoltage and power frequency overvoltage. At the triple point of high voltage apparatus, surface discharge occurs easily. After the propagation of the surface discharge, charge is accumulated on the insulation surface [1-5]. This residual charge will greatly influence the onset and the development of the subsequent discharge [6, 7]. It is also called “memorial effects [8]”. Many researchers have investigated partial discharge under dc stress and impulse conditions and find that the discharge is a complex and stochastic process [9, 10], but the stochastic behavior is inherently governed by memory effects [11]. The authors have developed charge measuring systems with a Pockels device and an electrostatic probe, and have measured the potential distribution on the insulator with the propagating surface discharge [12, 13] and investigated the fine structure of each surface discharge [14].

In this paper, surface discharges on the PET (Polyethylene terephthalate, relative permittivity: 3.2 at 1 MHz) film are observed with high speed cameras and measured by an electrostatic probe. From the photographs and potential distribution figures, the influence of the residual charge on the propagation characteristics of surface discharge, including the propagation pattern, length and velocity, discharge current and potential gradient are studied.

6.2 Experimental setup

The investigations have been performed in a cylindrical insulator configuration as shown in Fig. 6.1. There are two ring electrodes and one rod back electrode. The

distance between two ring electrodes is 300 mm. The diameter and the length of the rod back electrode are 29.6 mm and 600 mm, respectively. There is a 0.2 mm-thick PET film layer as the insulator between the pair of ring electrodes and the grounded back electrode.

The experiment is carried out in atmosphere and the application voltage is 1.2/50□μs standard lightning impulse. Two cameras are used to observe the discharge. One is the high speed video camera (Phantom, Vision Research Inc.) and the other is ultra high speed framing and streak camera (Imacon 468, NAC).

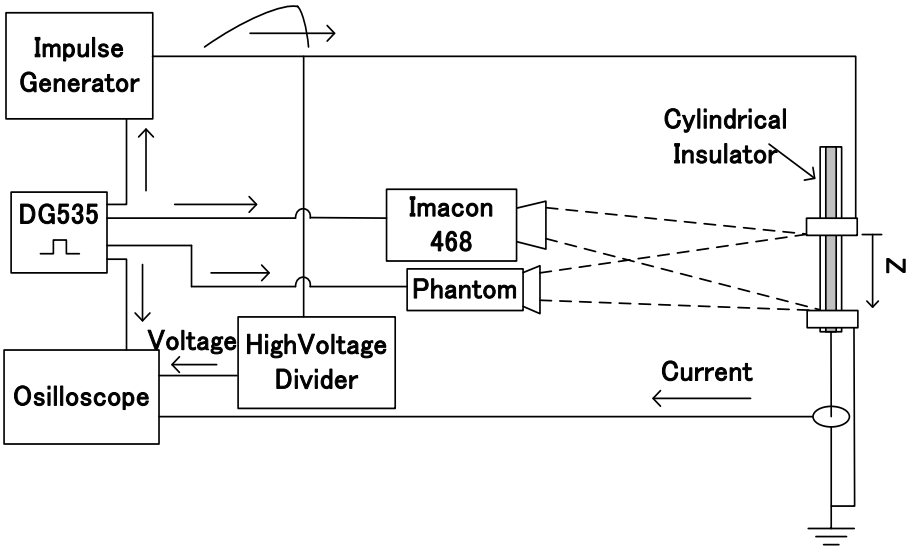

(a)

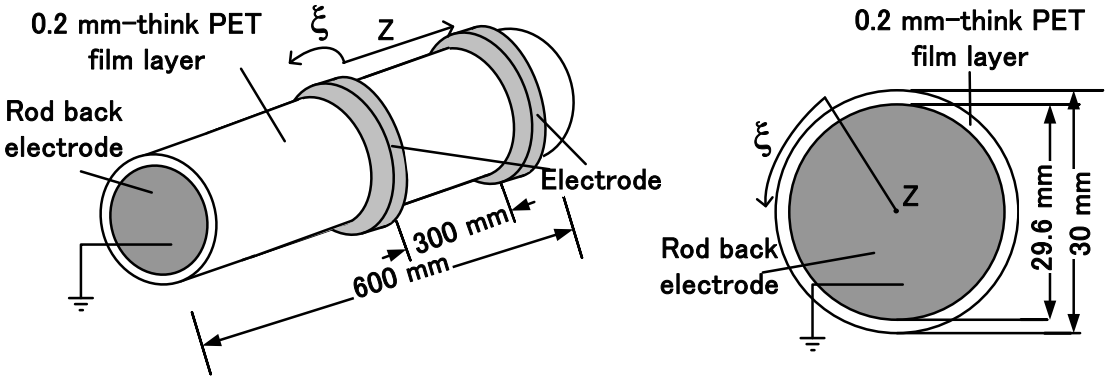

(b)

Fig. 6.1 Experimental setup, (a) Schematic of experimental setup and (b) Structure of cylindrical insulator

6.3Experimental Result and Discussion

6.3.1 Propagation pattern

The exposure time of the high speed video camera is set to 66 □μs. Typical discharge images taken by the high speed video camera under the application of standard lightning impulse voltage of 17.6 kV in its peak value are shown in Fig. 6.2: Figure 6.2(a) shows the scope area taken by phantom, which is 48 mm×96 mm; (b) is negative discharge on the clear insulator surface and (c) is positive discharge with the residual charge of (b); (d) is positive discharge on the clear insulator surface and (e) is negative discharge with the residual charge of (d).

Negative discharge on the clear insulator surface propagates from the high-voltage electrode to the grounded electrode without branches, while positive discharge on the clear insulator consists of many small branches. The path of a discharge after an opposite polarity discharge is similar with the previous one. And the discharge pattern is also influenced by the residual charge of the previous discharge: The negative discharge after the positive discharge consists of some branches as shown in Fig. 6.2(e), although not as much as those of the previous one as shown in Fig. 6.2(d).

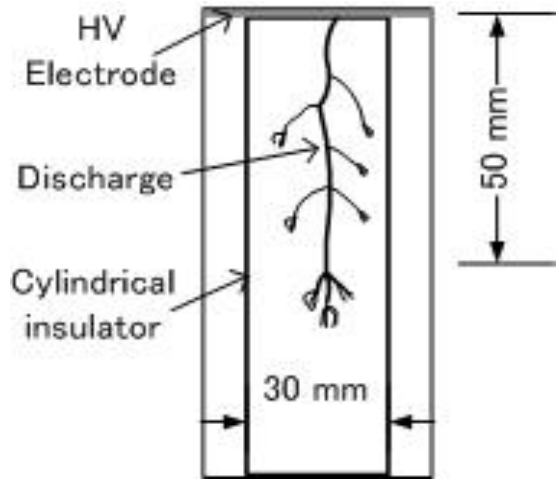

(a)

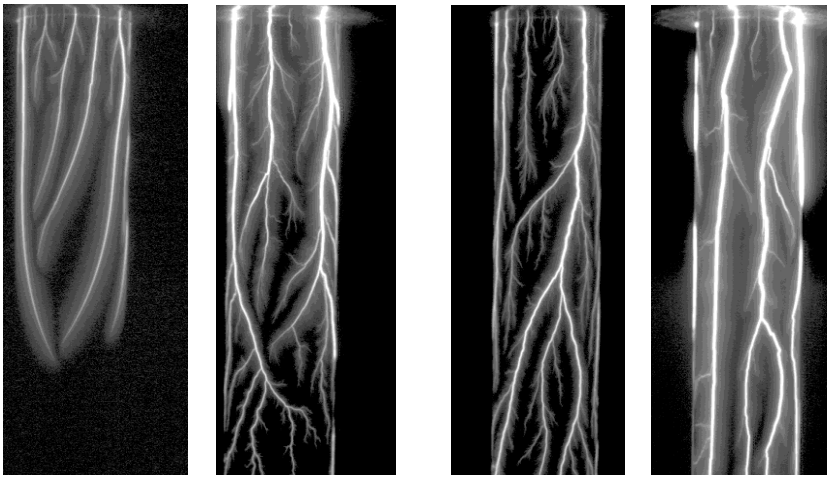

(b) (c) (d) (e)

Fig. 6.2 Typical discharge images under 17.6 kV; (a) scope area, (b) negative discharge on clear insulator, (c) positive discharge with residual charge of (b), (d) negative discharge with residual charge of (c), (e) positive discharge with residual charge of (d).

6.3.2 Propagation distance

Changing the application voltage from 12kV to 18kV, the propagation length of the surface discharge is measured from the photographs. The results are shown in Fig. 6.3. P and N are positive and negative discharge on clear insulator surface, P-P and P-N are respectively positive discharges after a positive discharge and a negative discharge, N-P and N-N are respectively negative discharges after a positive discharge and a negative discharge.

It can be seen that on the clear insulator surface the length of negative discharge, L_N, is much shorter than that of the positive discharge, L_P. But the length of the negative discharge with the residual charge of the previous positive discharge, $L_{N\text{-}P}$, is almost the same as the positive discharge with the residual charge of the previous negative discharge, $L_{P\text{-}N,}$ and almost the same as L_P.

As shown in Fig. 6.3, the length of discharge under different conditions almost linearly increases with the increase of the application voltage. The length of the negative discharge on the clear insulator, L_N, can be described by:

$$L_N = 11.6V - 126 \tag{6.1}$$

where V is the application voltage in kV.

In Fig. 6.3, because of the dispersion of the measured data, the length of the positive discharge on the clear insulator, L_P, the length of the negative discharge with the residual charge of the previous positive discharge, $L_{N\text{-}P}$, and the length of the positive discharge with the residual charge of the previous negative discharge, $L_{P\text{-}N}$, are almost the same and can be described by:

$$L_P \approx L_{N\text{-}P} \approx L_{P\text{-}N} = 16.8V - 168 \tag{6.2}$$

But when the impulse voltage is consecutively applied 25 times with changing the polarity, the propagation length of surface discharge increases with the number of the voltage application, as shown in Fig. 4, and it hardly converges. The averaged increment of the discharge length of a positive discharge after a negative discharge is much longer than that of a negative discharge after a positive discharge. It suggests that the propagation length of the positive discharge is more affected by the residual charge of the previous discharge.

The images of the 25 times serial surface discharge are shown in Fig. 6.5: odd

number images are positive discharge and even number images are negative discharge. The range of the image is 48 mm × 130 mm. After the propagation of a surface discharge, a back discharge will occur in the area near the HV electrode, therefore, only the front parts of surface discharge are compared.

The propagation path and the pattern of a negative surface discharge after a positive surface discharge is influenced by the residual charge of the positive surface discharge; The negative discharges shown in Figs. 6.5 (b) and Figs. 6.5 (d) propagate with some branched and their propagation paths are similar with the previous positive surface discharges shown in Figs. 6.5 (a) and 6.5 (b). On the other hand, the propagation path and the pattern of a positive surface discharge are less influenced by the residual charge of a previous negative surface discharge. The positive discharge shown in Fig. 6.5 (c) consists of small branches and its path differs from that in Fig. 6.5 (a).

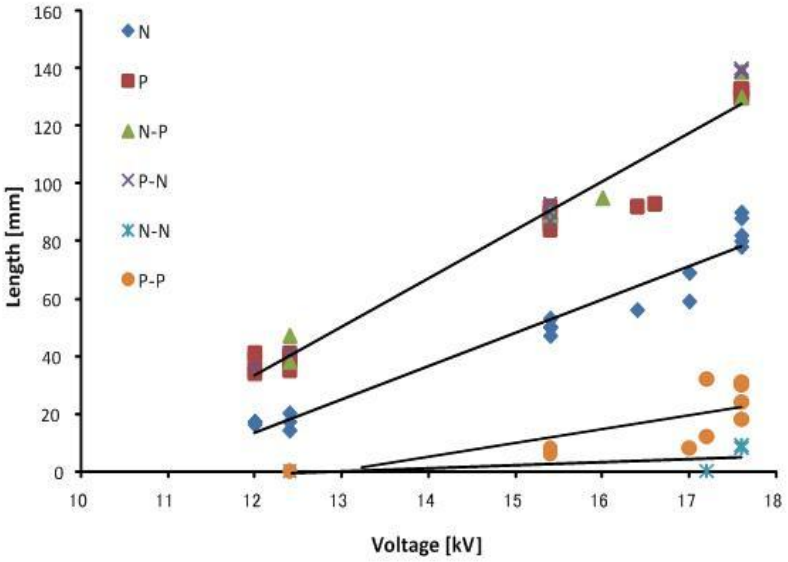

Fig.6.3 Discharge length under different conditions

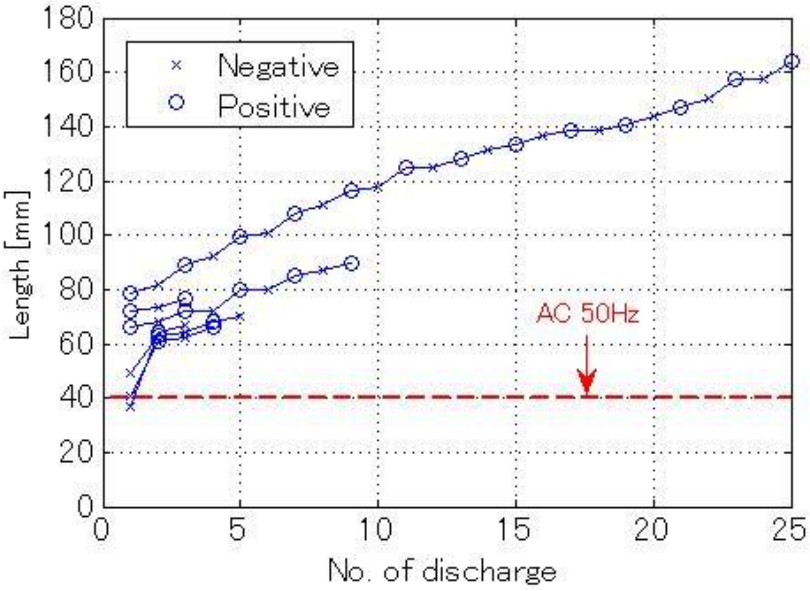

Fig. 6.4 Growth of discharge length of serial application of impulse voltage with changing its polarity

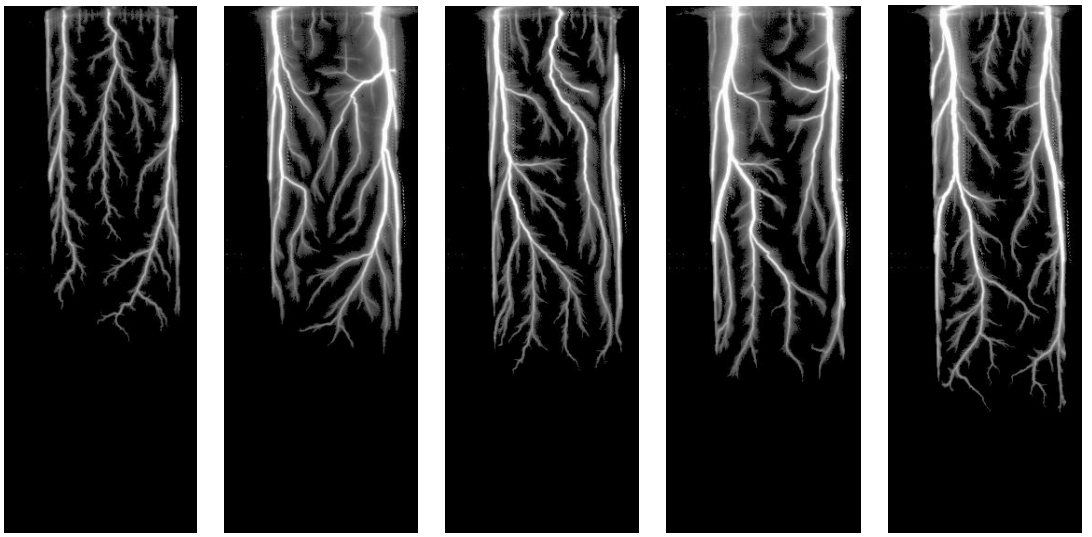

(a) (b) (c) (d) (e)

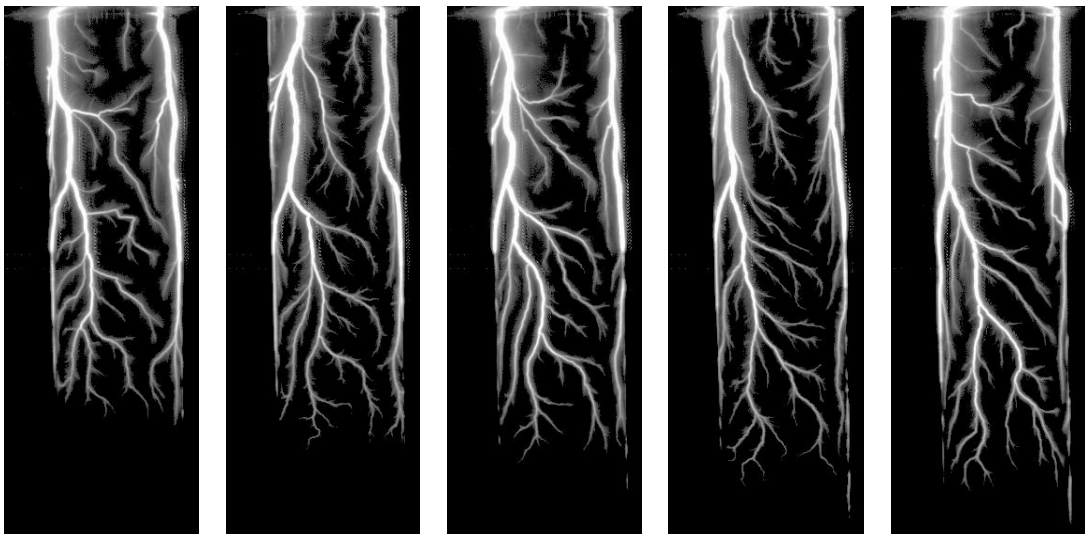

(f) (g) (h) (i) (j)

(k) (l) (m) (n) (o)

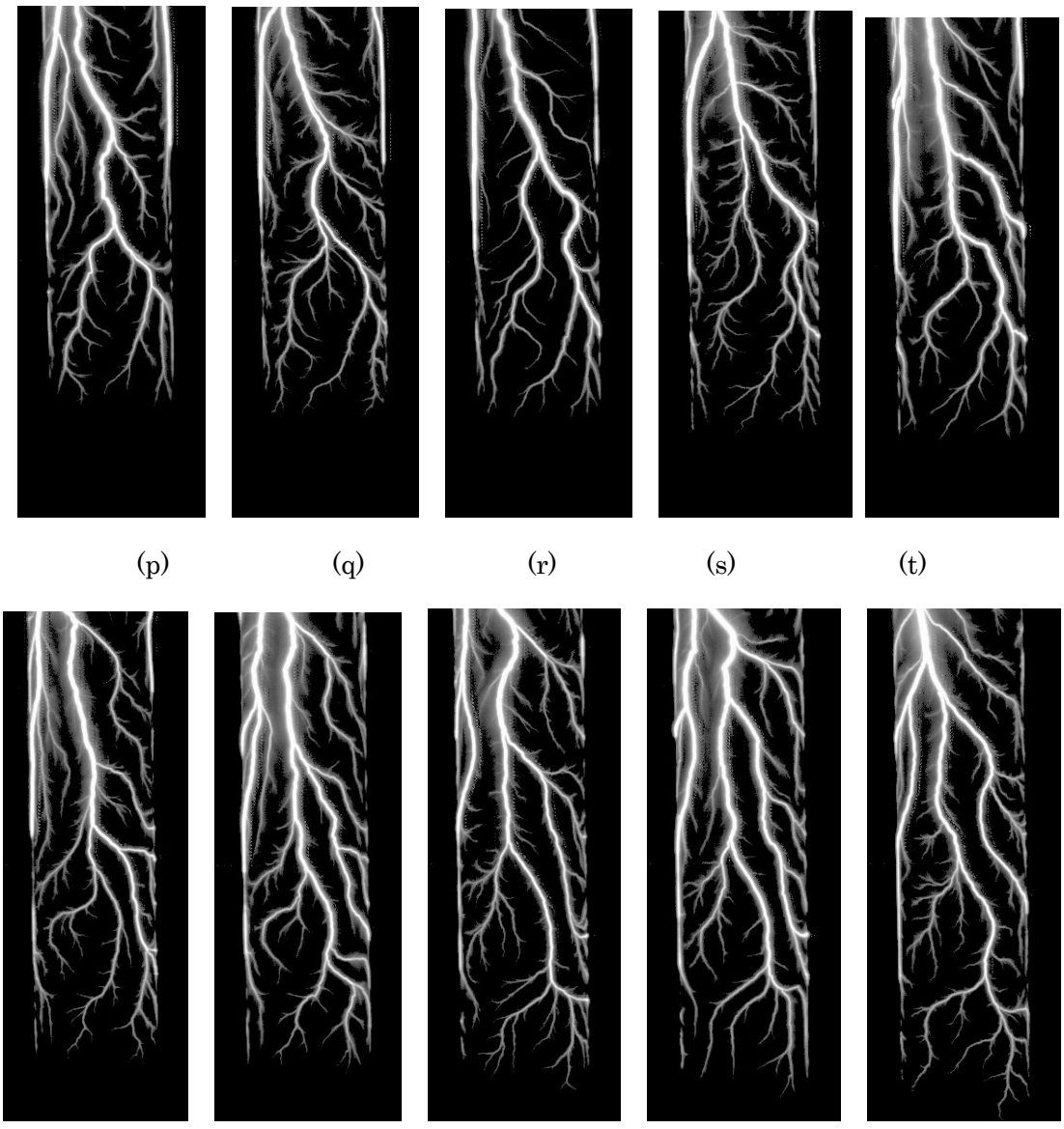

Fig. 6.5 Images of 25-times consecutive surface discharge; (a) No. 1, (b) No. 2, (c) No. 3, (d) No. 4, (e) No. 5, (f) No. 6, (g) No. 7, (h) No. 8, (i) No. 9, (j) No. 10, (k) No. 11, (l) No. 12, (m) No. 13, (n) No. 14, (o) No. 15, (p) No. 16, (q) No. 17, (r) No. 18, (s) No. 19, (t) No. 20, (u) No. 21, (v) No. 22, (w) No. 23, (x) No. 24, (y) No. 25.

6.3.3 Propagation speed

As mentioned in the previous subsection, the electric field along the discharge propagation path is changed by the residual charge. To study the influence of the residual charge on the discharge occurrence time and the propagation speed, the framing and streak images of the surface discharges with/without the residual charge are taken by Imacon 468.

Figures 6.6 (a), 6.6 (b), and 6.6 (c) show the voltage and current waveforms, streak image, and framing images for a positive surface discharge on the clear insulator, respectively. The application voltage is positive impulse of +15.4kV in its peak value, and the gate exposure timing for each frame and streak duration are also illustrated in Fig. 6 .6 (a).

With the residual charge of this positive surface discharge on the insulator surface, negative impulse voltage of -15.4kV in its peak value is applied and the voltage and current waveforms, framing image, and streak image of the subsequent negative surface discharge are monitored as shown in Fig. 6.7.

In the same manner, the negative surface discharge on the clear insulator under the application of -15.4kV impulse voltage is monitored as shown in Fig. 6.8. And the subsequent positive surface discharge with the residual charge of the negative discharge shown in Fig. 6.8 is also monitored as shown in Fig. 6.9.

The beginning of illumination is regard as the start of discharge. The time between the origin of impulse voltage and the beginning of illumination is regarded as delay time. The gradient in streak images is regarded as propagation speed. From these images, the delay time, the last time, the propagation length and the propagation speed are calculated and listed in Table 6.1. With the residual charge of different polarity, the delay time and last time are shortened, and the speed of discharge is greatly accelerated.

Table 6.1
Propagation surface discharge under different conditions

Type	Delay time (μs)	Last time (μs)	Length (mm)	Speed (mm/μs)
P	0.40	1.0	84	80
P-N	0.16	0.38	87	400
N	0.40	1.0	53	50
N-P	0.38	0.34	89	260

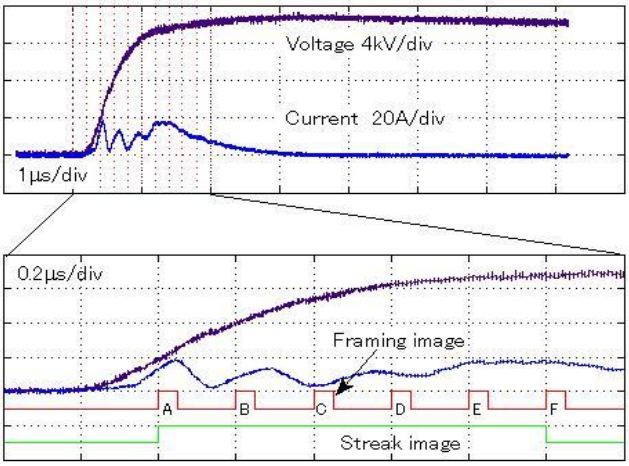

(a) Voltage and current waveforms

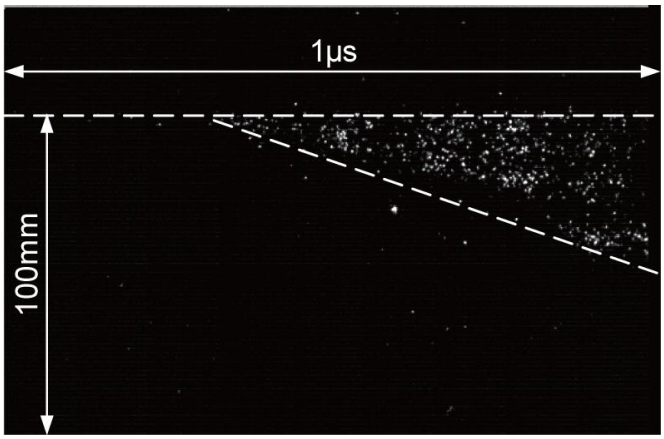

(b) Streak image

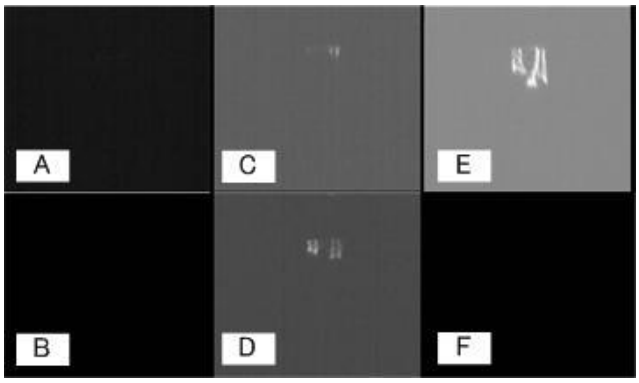

(c) Framing image

Fig.6.6 Voltage and current waveforms, streak image, and framing images of surface discharge under +15.4kV application on clear insulator surface

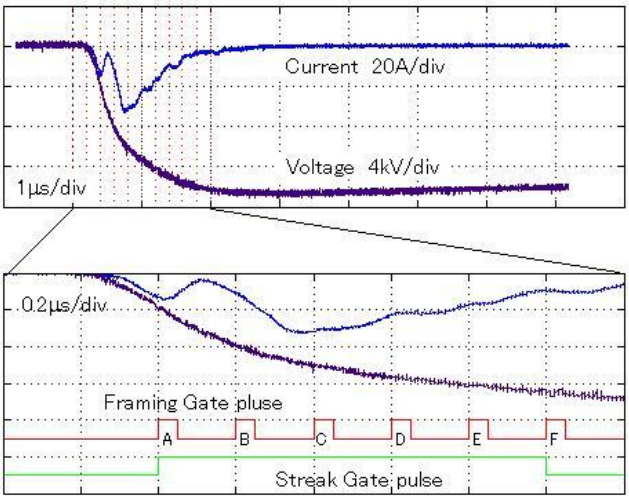

(a) Voltage and current waveforms

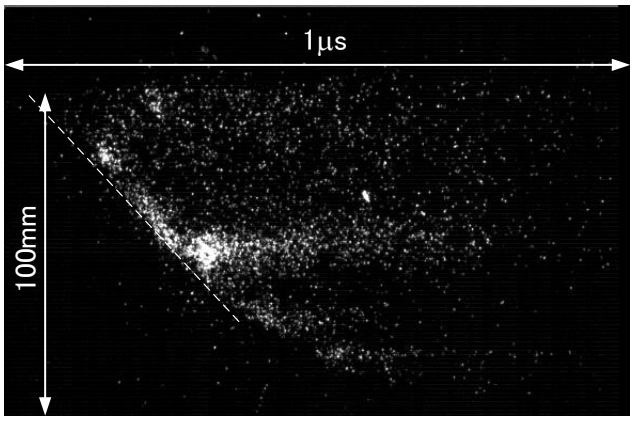

(b) Streak image

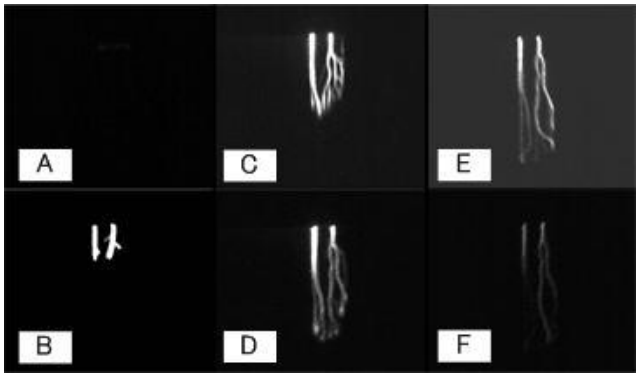

(c) Framing image

Fig.6.7. Voltage and current waveforms, streak image, and framing images of surface discharge under -15.4kV application voltage on the insulator surface with residual charge of +15.4kV application

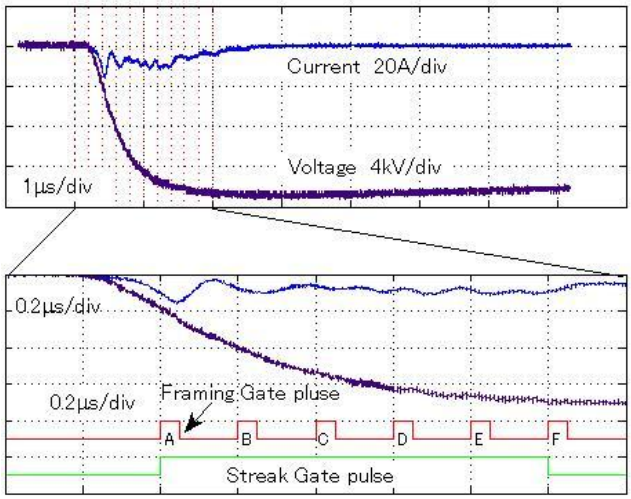

(a) Voltage and current waveforms

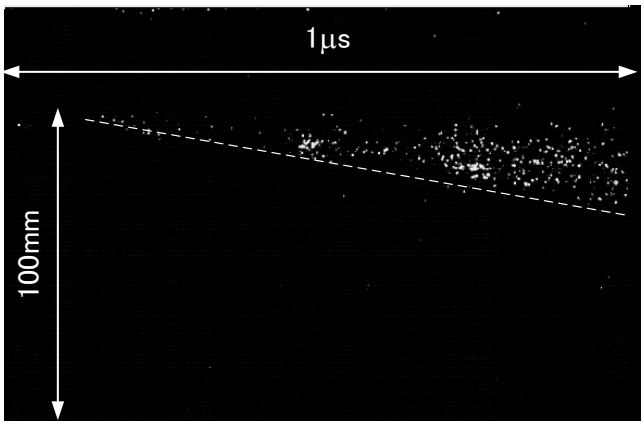

(b) Streak image

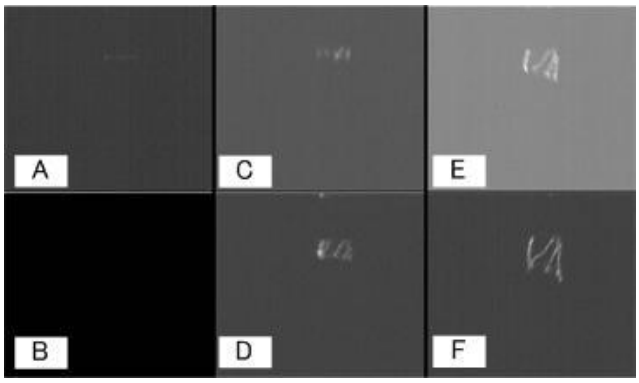

(c) Framing image

Fig.6.8 Voltage and current waveforms, streak image, and framing images of surface discharge under -15.4kV application on clear insulator surface

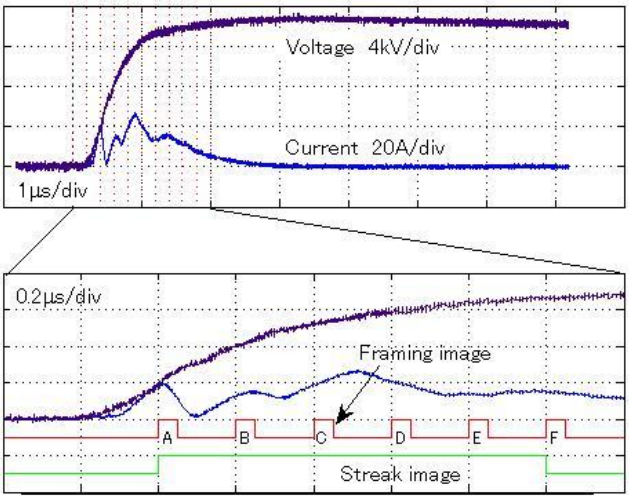

(a) Voltage and current waveforms

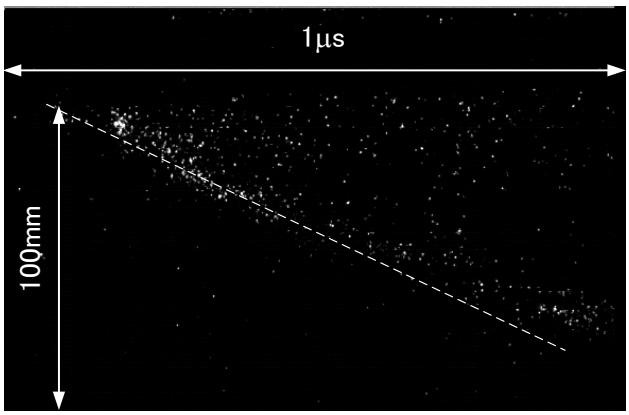

(b) Streak image

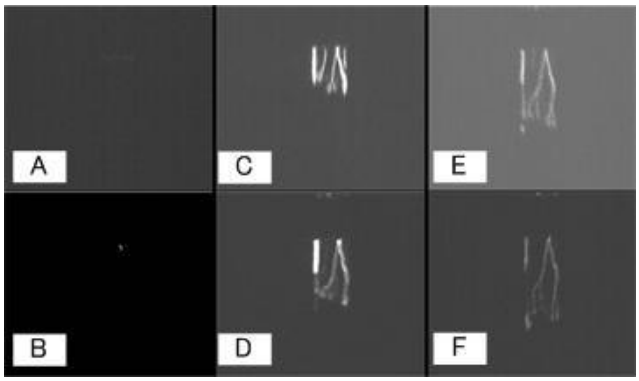

(c) Framing image

Fig. 6.9. Voltage and current waveforms, streak image, and framing images of surface discharge under +15.4kV application voltage on the insulator surface with residual charge of -15.4kV application

6.3.4 Surface discharge under AC voltage

Since the polarity of AC voltage also changes continuously, the discharge developed by 50 Hz AC voltage application is studied to compare with the discharge under consecutive impulse application with changing the polarity. Figure 6.10 shows voltage and current waveforms. A series of current pulses flow at the same time of discharge occurs. Almost all current pulses are observed during 0 to 5 ms and 10 to 15 ms, where the magnitude of the voltage is increasing.

Using high speed video camera, the discharge images are taken at the speed of 1 frame per 1 ms with and exposure time of 0.99 ms. In one cycle, 21 frames of images are taken at t = 0, 1, 2, …, 20 ms respectively, and are named Frame No. 0, No. 1, No. 2, …, No. 20, as shown in Figures 6.11(a), (b), …, (u). The observed area of the image is 48 mm × 96 mm.

The maximum discharge length is 40 mm, which is almost equal to the length of negative discharge on clear surface and is only 1/4 of the 25th consecutive impulse discharge shown in Fig. 6.4. It has been reported that the flashover voltage on a 0.75 mm-long insulator under 1 MHz-voltage application decreases to less than 1/10 of that under 50 Hz-voltage [15, 16]. The short propagation length of the AC-surface discharge measured in this study coincides qualitatively with these reports.

It is possible to explain this phenomenon as follows: the rising slope of AC voltage is very long compared with the propagating time of a surface discharge under an impulse voltage application which is shorter than 2 μs. So, where the voltage is still very low, the initial electrons are supplied from the electrode or air and a streamer discharge starts to propagate. Because of the low voltage, the propagation length of this streamer discharge is short. When the voltage increases and reaches a certain value, a surface leader is formed and propagates through the previous streamer discharge region. Because of the suppression effects of the residual charge with the same polarity on the insulator surface, this subsequent leader hardly propagates a long length.

It is possible to explain this phenomenon as follows: comparing with the last time of surface discharge under impulse application voltage, which is about 1 μs, the rising slope of AC voltage is very long. So, in the 0-π/2 region, when the instantaneous application voltage is still very low, the primary electrons come into being, surface discharge start to propagate. Because of the low instantaneous application voltage, the length of discharge is very short, (Fig. 6.11(a)). When the instantaneous application voltage rise to high enough, the surface discharge will start to propagate forward again and across the brush-like discharge region, but because of the suppress effects of the residual charge on the surface, so it can not propagate very long, (Fig. 6.11(a)). For the

same reason, the $L_{N\text{-}N}$ and $L_{P\text{-}P}$ are very short (as shown in Fig. 6.3). In the π-$3/2\pi$ region, just like the discharge happens in the $\pi/2$ region, when the instantaneous voltage is still low, discharge happens, some of the charge is absorbed by the charge of different polarity produced in the 0-$\pi/2$ region.

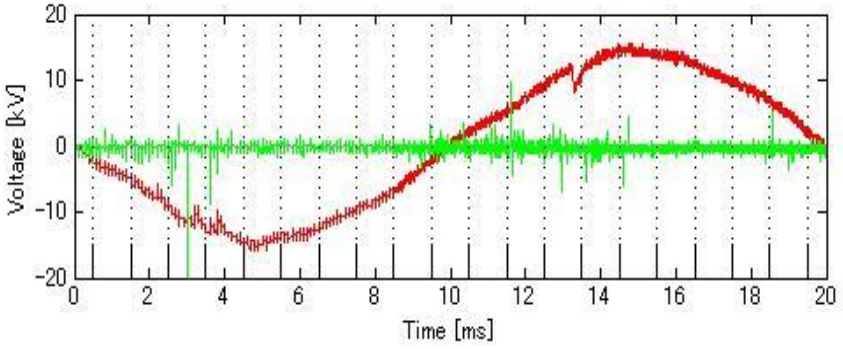

Fig. 6.10. Applied AC voltage and discharge current

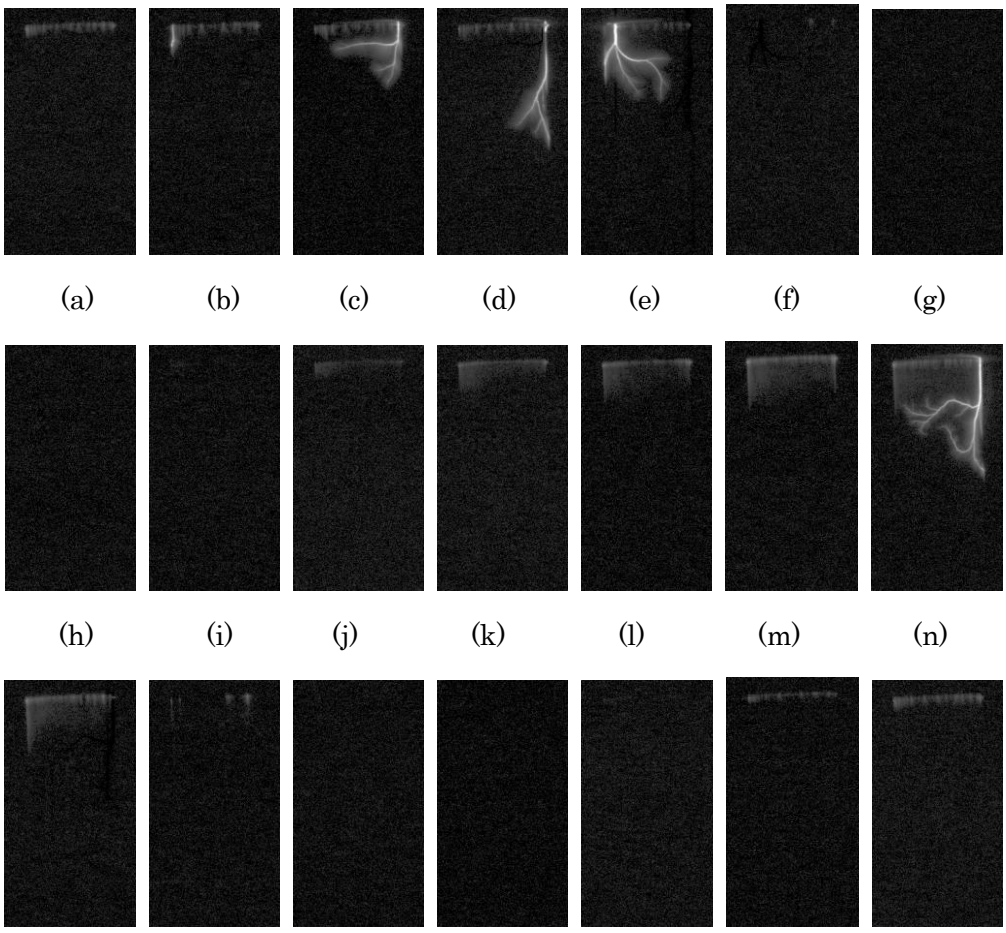

Fig. 6.11. Images of AC discharge in one cycle; (a) No. 0, (b) No. 1, (c) No. 2, (d) No. 3, (e) No. 4, (f) No. 5, (g) No. 6, (h) No. 7, (i) No. 8, (j) No. 9, (k) No. 10, (l) No. 11, (m) No. 12, (n) No. 13, (o) No. 14, (p) No. 15, (q) No. 16, (r) No. 17, (s) No. 18, (t) No. 19, (u) No. 20.

6.3.5 Propagation model

After discharge, the potential distribution above the insulator surface is measured by electrostatic probe (Trek 341B), as shown in Fig. 6.12. Since the insulator is very thin, the potential distribution agrees with the charge density distribution. The charge density can be approximately calculated by [17, 18]

$$\sigma = C \times V , \tag{6.3}$$

where σ is the charge density distribution, C is the capacitor of the insulator and V is the potential distribution.

The typical charge density distribution under +15.4 kV impulse voltage is shown in Fig. 6.13 (a), and the maximum value in the black-rectangle is shown in Fig. 6.13 (b). Fig. 6.14 is the typical charge density distribution under -15.4 kV impulse voltage.

According to the previous potential measurement results, the potential decrement along the pipe axis can be divided into two parts: leader part and streamer part. In the leader part, it decreases at about 0.6 kV/cm; while in the streamer part, it decreases with a speed of 3.3 kV/cm [18].

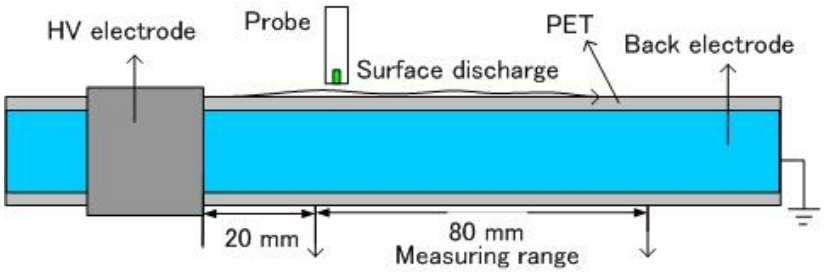

Fig. 6.12 Measurement of surface discharge

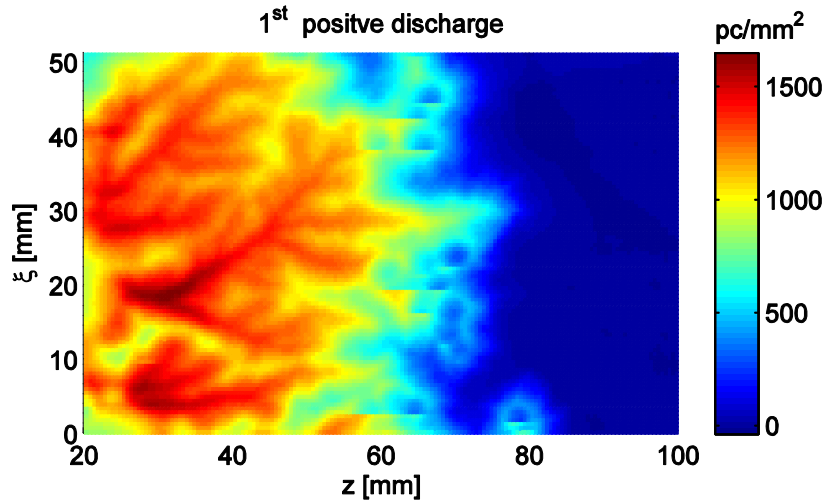
1st positve discharge
pc/mm2
1500
1000
500
0
50
40
30
20
10
0
ξ [mm]
20
40
60
80
100
z [mm]

(a)

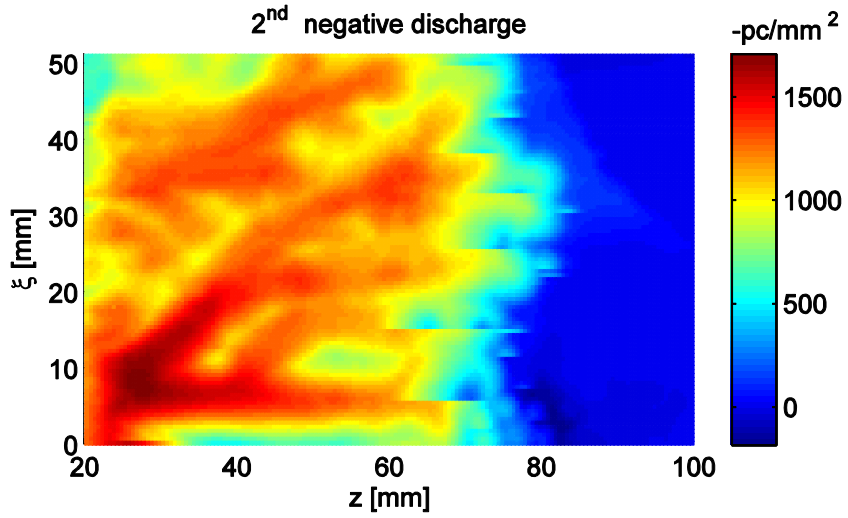
2nd negative discharge
-pc/mm 2
1500
1000
500
0
50
40
30
20
10
0
ξ [mm]
20
40
60
80
100
z [mm]

(b)

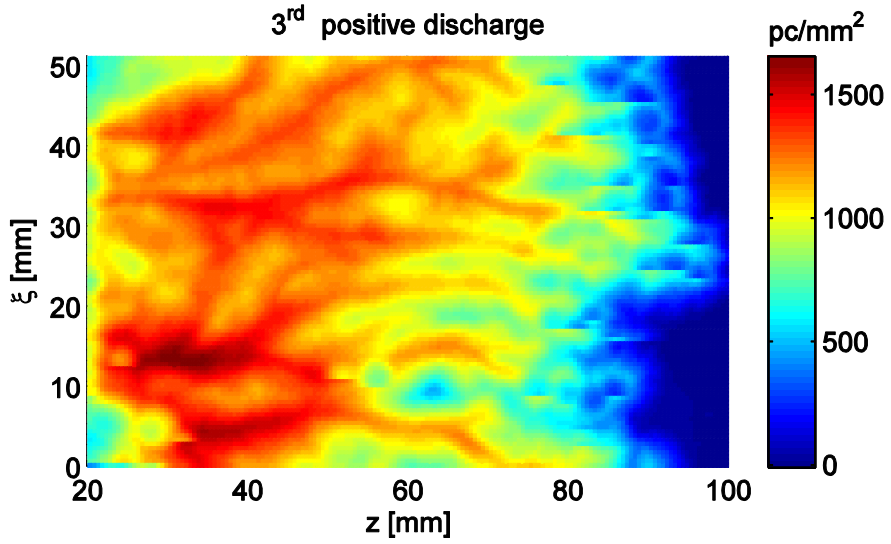

(c)

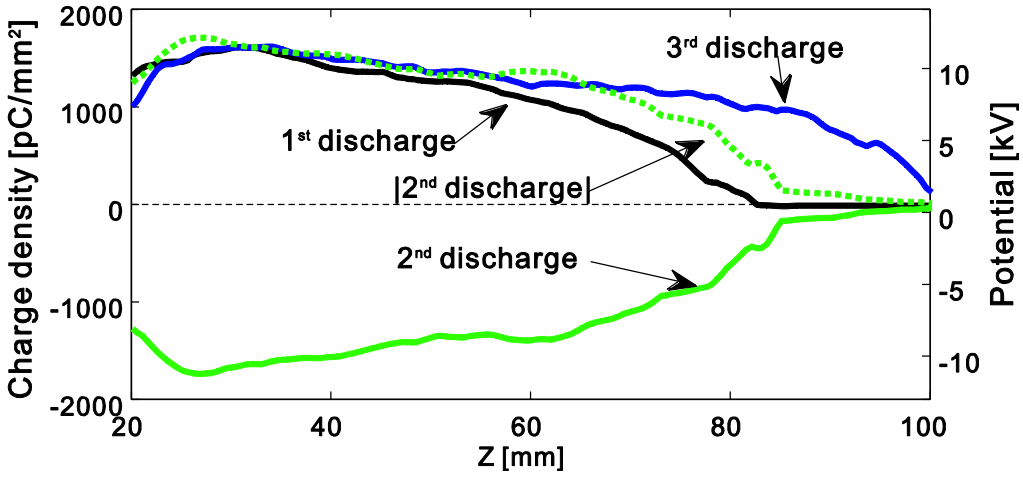

(d)

Fig. 6.13 Charge distribution under positive-negative-positive impulse application voltage; Charge distribution under the (a) 1st positive discharge and (b) 2nd negative discharge (c) 3rd positive discharge (d) the maximum/minimum charge density and potential along z axis.

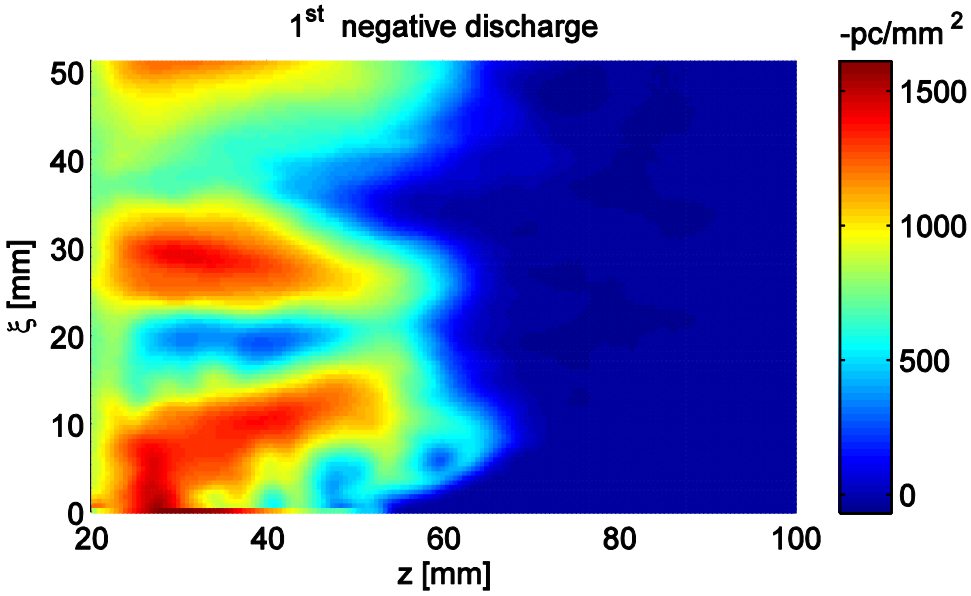
1st negative discharge
-pc/mm 2
1500
1000
500
0
50
40
30
20
10
0
ξ [mm]
20
40
60
80
100
z [mm]

(a)

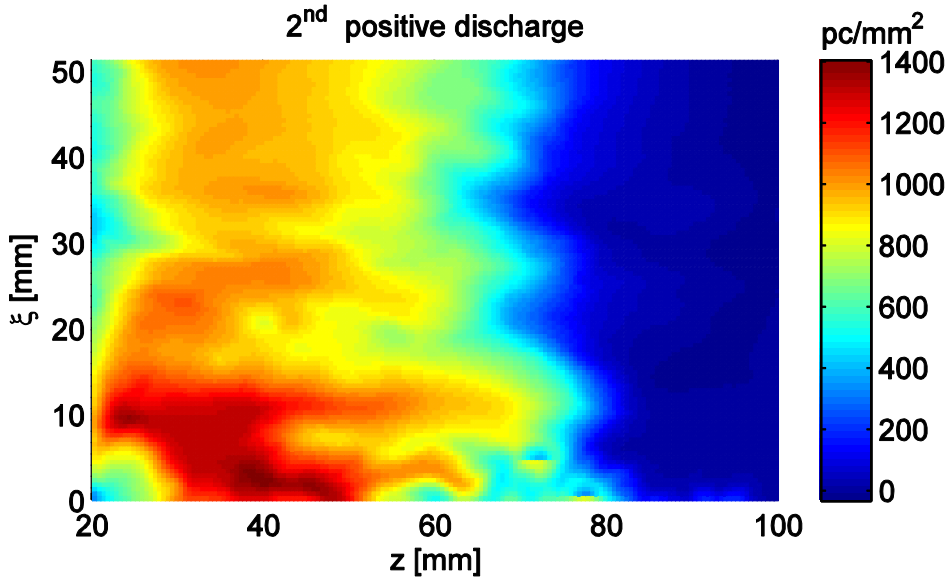
2nd positive discharge
pc/mm2
1400
1200
1000
800
600
400
200
0
50
40
30
20
10
0
ξ [mm]
20
40
60
80
100
z [mm]

(b)

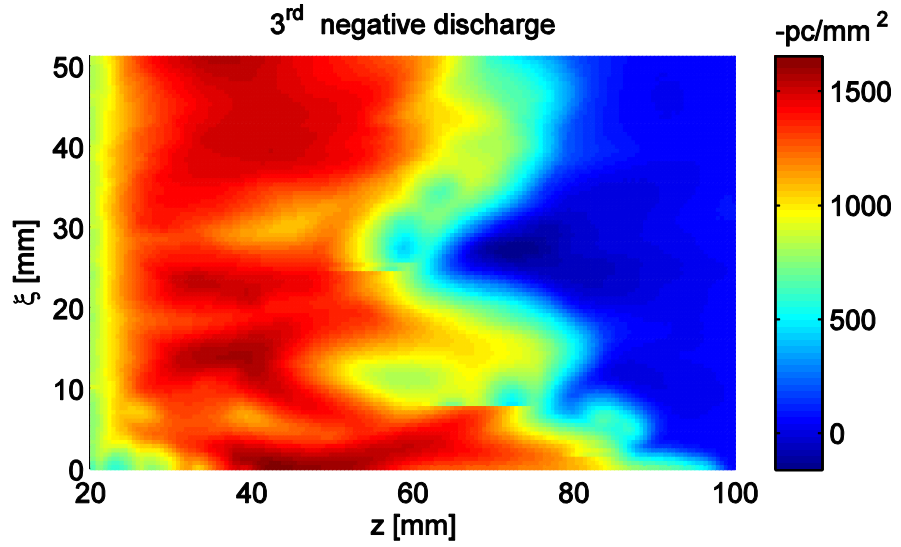

(c)

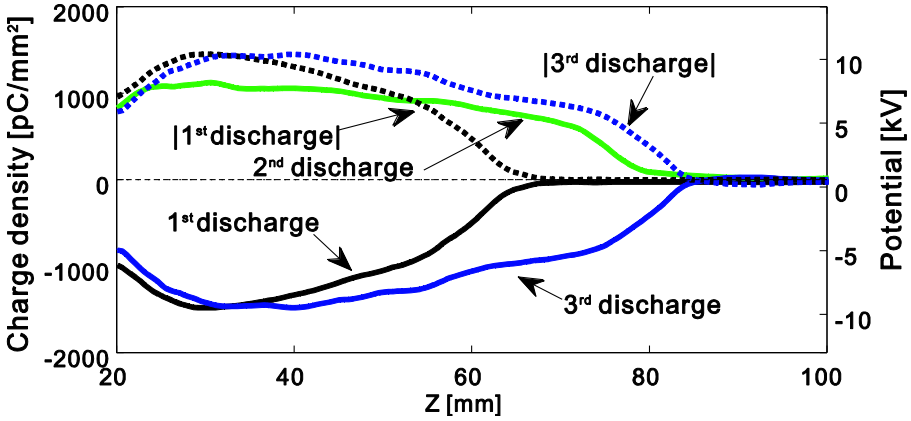

(d)

Fig. 6.14 Charge distribution under negative-positive- negative impulse application voltage; Charge distribution under the (a) 1st negative discharge and (b) 2nd positive discharge (c) 3rd negative discharge (d) the maximum/minimum charge density and potential along z axis.

6.3.6 Discussion

According to the images of discharge, with the electrode configuration described in Fig. 6.1, the schematic of discharge propagation on clear insulator surface are shown in Fig. 6.15 [19], a leader looks like a thin channel propagate forward from the high voltage electrode. The average radius is less than one millimeter.

There is a charge cover around the leader channel. The charge produced by streamer in the streamer zone is accumulated in the cover. As the leader propagates, its head moves forward together with the point of inception of new streamers and with the streamer zone boundary. The earlier streamer and their surface charge do not move forward; as a result, the elongating leader is surrounded by a charge cover.

For the negative discharge, the electrons provided by the high voltage electrode, there are enough electrons emitted from the head to streamer zone, the streamer zone is big and glow is uniformly distributed, so, after discharge, residual charge is uniformly distributed on the surface of the insulator. While for the positive discharge, the electrons come from ionization in the streamer zone. When the electrical field is not very high, the ionization rate is not very high, so, the streamer zone is very small and the head is easy to pull through the streamer zone to move forward. That's why a positive leader propagates faster and longer than a negative leader under the same voltage.

The schematic of negative subsequent a positive discharge is shown in Fig. 6.16. After positive discharge, positive charge is accumulated on the insulator surface, where the residual charge is accumulated, positive potential is produced. When the subsequent negative discharge propagates to this place, the potential difference is greater than that on the clear insulator surface, so the discharge is intensified and easy to move forward along the trance of the former discharge. When the discharge propagates to the head place of the former discharge, the potential difference is still high than the necessary potential to propagate forward, so it can be propagate a little further than the former discharge. The principle is the same for the negative discharge after positive discharge.

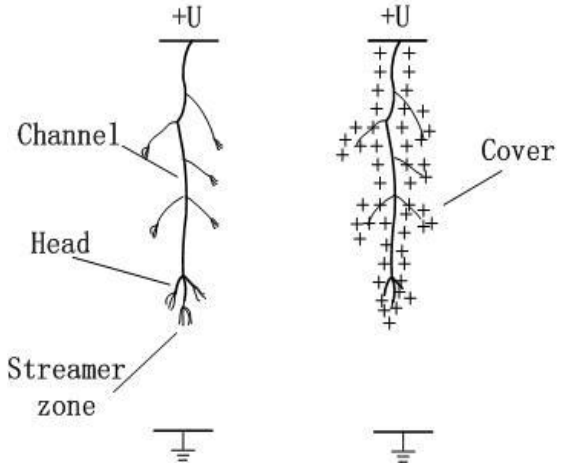

(a)

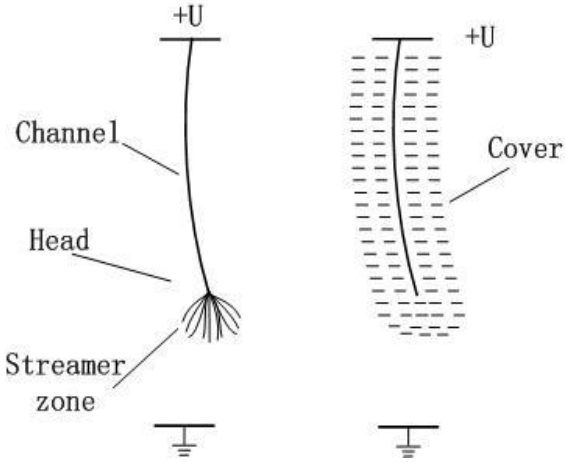

(b)

Fig.6.15. Schematic of discharge propagation on clear insulator surface; (a) positive discharge, (b) negative discharge.

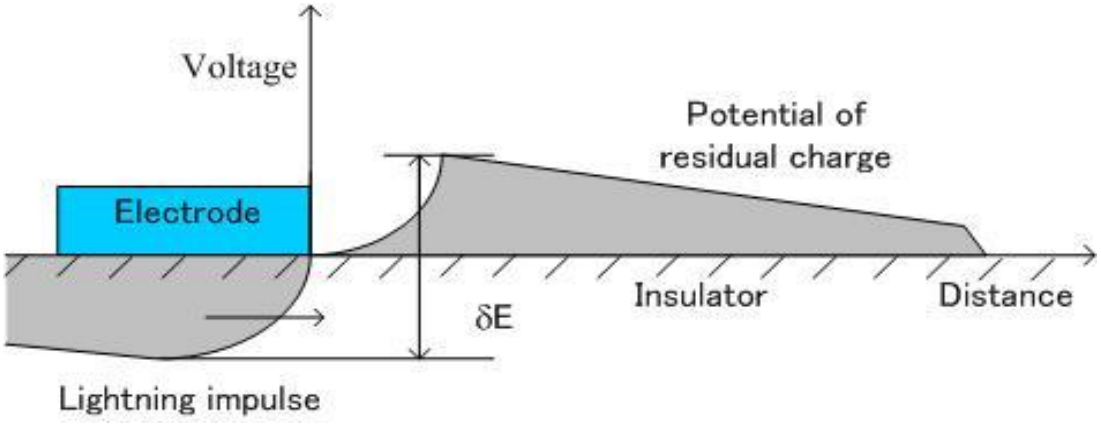

Fig.6.16. Schematic of negative discharge subsequent a positive discharge

6.4 Summary

In this chapter, the influence of residual charge, which is generated by a surface discharge, to the subsequent surface discharge is studied and the results are summarized as follows:

a) When consecutive impulse voltages are applied with changing the polarity, the propagation length of the surface discharge increases gradually and hardly converges. In such a condition, the potential gradient in the leader part decreases with the consecutive number of impulses, while that in the streamer part keeps constant.

b) With the residual charge of the positive surface discharge, the subsequent negative discharge propagates with branching and follows the path of the previous positive discharge.

c) The propagation velocity of the surface discharge becomes faster by the residual charge with the opposite polarity.

References

[1] W. Boeck, W. Taschner, J. Gorablciikow, G. F. Luxa and L. Mcntcii, " Insulating behavior of SF6 with and without solid insulation in case of fast transients," *GIGRE Report* 15-07, Paris, 1986.

[2] T.S. Sudarshan and R. A. Dougal, "Mechanism of surface flashover along solid dielectrics in compressed gases," *IEEE Trans. on Electrical Insulation,* Vol. 21, pp. 727-746, 1986.

[3] S. Tenbohlen and G. Schroder, "The influence of surface charge on lightning impulse breakdown of spacers in SF6," *IEEE Trans. on Dielectrics and Electrical Insulation,* Vol. 7, pp.241-246, 2000.

[4] M. Chiba, A. Kumada and K. Hidaka, "Inception voltage of positive streamer and its length on PMMA in air," *IEEE Trans. Dielectrics Electrical Insulation,* Vol.9, pp.118-23, 2002

[5] Y. Murooka, T. Takada and K. Hidaka, "Nanosecond surface discharge and charge density evaluation part I: review and experiments," *IEEE Electrical Insulation Magazine,* Vol. 17, pp.6-16, 2001.

[6] M. Yashima and E. Kuffel, "Breakdown characteristics of dielectric spacers with accumulated surface charge in SF6 under fast oscillating impulse voltage," Proc. Of

8th International Symposium on High Voltage Engineering, Yokohama, Japan, 1993, pp. 267-270.

[7] O. Farish and I. Al-Bawy, "Effect of surface charge on impulse flashover of insulators in SF6," *IEEE Trans. on Electrical Insulation,* Vol. 26, pp.443-452, 1991.

[8] Y. Zhu, T, Takada, K. Sakai and D. Tu, "The dynamic measurement of surface charge distribution deposited from partial discharge in air by pockels effect technique," *J. Phys. D: Appl. Phys.* Vol. 29, pp. 2892-2900, 1996.

[9] V. Brunt and S. Kulkdawala, "Stochastic properties of trichel-pulse corona: a non-Markoviam random poit process," *Phys. Riew. A,* Vol. 42, pp. 4908-4922, 1990.

[10] V. Brunt, M. Misakian and S. Kulkdawala, "Infulence of a dielectric barrier on the stochastic behavior of trichel-pulse corona," *IEEE Trans. on Electrical Insulation,* Vol. 26, pp. 405-415, 1990.

[11] Y. Zhu, T. Takada and D. Tu, "An optical charge measurement technique for studying residual charge distribution," *J. Phys. D: Appl. Phys.,* Vol. 28, pp. 1468-1477, 1995.

[12] A. Kumada, M. Chiba and K. Hidaka, "Potential Distribution Measurement of Surface Discharge Developing on Insulating Material," *Trans. IEE of Japan.* Vol. 120-B, No.1, pp.75-80, 2000.

[13] D. Tanaka, S. Matsuoka, A. Kumada and K. Hidaka, "Two-dimensional potential and charge distributions of positive surface streamer", *J. Phys. D: Appl. Phys.*, Vol. 42 075204 (6pp), 2009.

[14] A. Kumada, S. Okabe, K. Hidaka, "Residual Charge Distribution of Positive Surface Streamer", *J. Phys. D: Appl. Phys.*, Vol.42, pp.1-8, 2009.

[15] IEC 60664-4:2005, "Insulation coordination for equipment with low-voltage system-part4: Consideration of high-frequency voltage stress."

[16] H. Suhr, "Evaluation of the influencing factors on the breakdown voltage of thin insulating films" (in German), Disseratation, Techische Universitat Berlin, 1961.

[17] T. Takuma, M. Yashima, T. Kawamoto, "Principle of surface charge measurement for thick insulating specimens", IEEE Trans. on Dielectrics and Electrical Insulation, Vol. 5, No. 4, pp. 497-504, 1998.

[18] A. Kumada, S. Okabe, K. Hidaka, "Influences of probe geometry and experimental errors on spatial resolution of surface charge measurement with electrostatic probe", IEEE Transactions on Dielectrics and Electrical Insulation, Vol. 12, No. 6, pp. 1172 – 1181.

[19] J. Deng, S. Matsuoka, A. Kumada and K. Hidaka, "Residual charge density

distribution measurement of surface discharge on cylindrical insulator", International conference on electrical engineering, Shenyang, China, I9FP0310, 2009.

[20] S. Larigaldie, “Spark propagation mechanisms in ambient air at the surface of a charged dielectric. I. Experiment: The main stages of the discharge”, J. Appl. Phys. Vol. 61. No.1, 1987, pp.91-101.

[21] S. Larigaldie, “Spark propagation mechanisms in ambient air at the surface of a charged dielectric. II. Theoretical modeling”, J. Appl. Phys. Vol. 61. No.1, 1987, pp.102-108.

Chapter 7

Conclusions

Surface discharge on dielectric materials is an important factor which affects the insulating performance of electrical apparatus. With the increase of the applied voltage, the surface discharge transforms from streamer to leader and easily propagates a long length.

To study the development process of leader discharge, the following experiments have been arranged:

A) An impulse generator using semi-conductor switch is assembled. This IG generates the standard lightning impulse voltage and is easily controlled.

B) A surface potential measuring system is constructed and the residual charge distributions on insulator pipes are measured with this system. The spatial resolution reaches 1.8 mm for measuring a 5 mm-thick PMMA pipe, 0.30 mm for measuring a two-layer structure pipe and 0.28 mm for measuring a 200 μm-thick PET pipe.

C) By utilizing Tikhonov's regularization technique in Fourier domain, the inverse calculation form the measured potential distribution to the charge distribution requires less computational load and becomes stable.

D) For measuring highly charged insulator with the residual charge of a surface leader, two-layer structure pipe is introduced. The pipe has an internal layer of low resistivity, which can be grounded during the measuring process.

With the experimental setups and methods described above, the propagation characteristics of surface discharge under impulse and AC application voltage are investigated. The results of AC-discharge dynamics, which are investigated with a high speed video camera, are summarized as follows:

E) With increasing the voltage, leader discharges are recognized, whose occurrences concentrate in the negative half-cycles of AC voltage application. When the voltage is increased high enough, positive leader discharge also occurs.

F) There is little difference between the maximum propagation length of the positive leader and that of the negative leader. As later described in the item K), the propagation patterns of these leader discharges become similar with each other because of the

residual charge, and, therefore, the maximum propagation length hardly depends on the polarity of discharge.

G) As reported in the relevant studies, it is observed that the intrinsic capacitance of insulating materials has influence on the final discharge length. When the intrinsic capacitance is large, the leader discharges occur at a lower voltage, and the discharge easily propagates over a long distance.

H) The maximum length of discharge L_{MAX} under AC application voltage can be denoted by

$$L_{MAX} \propto V_p^{\ n} \quad , \tag{7.1}$$

where V_p is the amplitude of AC voltage, and n is 1.5 - 3.3.

The results of the impulse-discharge characteristics are summarized as follows:

I) The positive discharge length is longer than the negative one. The propagation length of an impulse surface discharge is almost three times as long as that of an AC discharge under the same peak voltage.

J) The potential gradients in the leader part and the streamer part are measured. For a positive discharge, the potential gradients in the leader part and the streamer part of a positive discharge are 0.15 - 0.2 kV/mm and 1.0 - 1.2 kV/mm, respectively. Those for a negative discharge are 0.15 - 0.2kV/mm and 1.0 - 1.6 kV/mm, respectively. Taking the spatial resolution of the measuring system into account, it can be said that these values agree with the reported values obtained by using Lichtenberg figure technique and Pockels sensing technique.

To evaluate the influence of residual charges on the propagation characteristics of surface discharge, including the propagation pattern, length and velocity, discharge current and potential gradient, are studied and the results are summarized as follows:

K) With the residual charge of a positive surface discharge, the subsequent negative discharge propagates with branching and follows the path of the previous positive discharge. In other words, there becomes little difference between propagation patterns of a positive discharge and a negative discharge.

L) The propagation velocity of discharge is increased due to the residual charge with the opposite polarity.

M) When consecutive impulse voltages are applied with changing the polarity, the propagation length of the discharge increases gradually and hardly converges. In such a condition, the potential gradient in the leader part decreases with the consecutive

number of impulses, while that in the streamer part keeps constant.

List of Publications

Journals

[1] J. Deng, S. Matsuoka, A. Kumada, K. Hidaka, "The influence of residual charge on surface discharge propagation", J. Physics D: Applied Physics. (Being accepted)
[2] J. Deng, S. Matsuoka, A. Kumada, K. Hidaka, "The propagation characteristics of surface leader", J. Physics D: Applied Physics. (To be submitted)

International Conferences and Symposiums

[1] J. Deng, L. Oliver, S. Matsuoka, A. Kumada, K. Hidaka, "Propagation of Surface Leader on PMMA Pipe", Regional Inter-university Graduate Conference on Electrical Engineering, Xi'an, China, 2008.
[2] J. Deng, S. Matsuoka, A. Kumada, K. Hidaka, "Measurement of Surface Leader on PMMA Pipe", The 9th SNU-UT joint seminar, Tokyo, 2009.
[3] J. Deng, S. Matsuoka, A. Kumada, K. Hidaka, "The influence of residual charge on surface leader propagation", The 10th SNU-UT joint seminar, Seoul, 2010.
[4] J. Deng, S. Matsuoka, A. Kumada, K. Hidaka, "Residual charge density distribution measurement of surface discharge on cylindrical insulator",International conference on electrical engineering, Shenyang, China, I9FP0310, 2009.
[5] J. Deng, S. Matsuoka, A. Kumada, K. Hidaka, "The influence of residual charge on surface discharge propagation", International conference on electrical engineering, Bussan, Korea, 2010.

Domestic Conferences and Symposiums

[1] I. Takahashi, J. Deng, S. Matsuoka, A. Kumada, K. Hidaka, "Measurement of Negative Streamer Charge Density with Electrostatic Probe", Conference of IEEJ, Toyama, 1-067, 2007.

[2] J. Deng, A. Kumada, “Propagation Phenomenon of Surface Discharge on the Surface of Pipe Insulator”, Secure-life Electronics Report of Tokyo global COE. Tokyo, 2007.
[3] J. Deng, L. Oliver, S. Matsuoka, A. Kumada, K. Hidaka, “The Development of Discharge on the Surface of Insulation Pipe”, Conference of IEEJ, KyuShu, 1-055, 2008.
[4] J. Deng, Z. Li, S. Matsuoka, A. Kumada, K. Hidaka, “Residual charge distribution Measurement of surface leader on cylindrical insulator”, Conference of IEEJ, Houkaido, 1-050, 2009.
[5] J. Deng, S. Matsuoka, A. Kumada, K. Hidaka, “The influence of residual charge on surface leader propagation”, Conference of IEEJ, Tokyo, 1-076, 2010.